Synapsin I (Protein I), a Nerve Terminal-Specific Phosphoprotein. I. Its General Distribution in Synapses of The Central and Peripheral Nervous System Demonstrated by Immunofluorescence in Frozen and Plastic Sections

P. DE CAMILLI, R. CAMERON, and P. GREENGARD

Section of Cell Biology and Department of Pharmacology, Yale University School of Medicine, New Haven, Connecticut 06510. Dr. De Camilli's present address is Consiglio Nazionale delle Ricerche, Center of Cytopharmacology and Department of Pharmacology, Università di Milano, Milano, Italy.

ABSTRACT Synapsin I (formerly referred to as protein I) is the collective name for two almost identical phosphoproteins, synapsin Ia and synapsin Ib (protein Ia and protein Ib), present in the nervous system. Synapsin I has previously been shown by immunoperoxidase studies (De Camilli, P., T. Ueda, F. E. Bloom, E. Battenberg, and P. Greengard, 1979, *Proc. Natl. Acad. Sci. USA*, 76:5977–5981; Bloom, F. E., T. Ueda, E. Battenberg, and P. Greengard, 1979, *Proc. Natl. Acad. Sci. USA* 76:5982–5986) to be a neuron-specific protein, present in both the central and peripheral nervous systems and concentrated in the synaptic region of nerve cells. In those preliminary studies, the occurrence of synapsin I could be demonstrated in only a portion of synapses. We have now carried out a detailed examination of the distribution of synapsin I immunoreactivity in the central and peripheral nervous systems. In this study we have attempted to maximize the level of resolution of immunohistochemical light microscopy images in order to estimate the proportion of immunoreactive synapses and to establish their precise distribution. Optimal results were obtained by the use of immunofluorescence in semithin sections (~1 μm) prepared from Epon-embedded nonosmicated tissues after the Epon had been removed.

Our results confirm the previous observations on the specific localization of synapsin I in nerve cells and synapses. In addition, the results strongly suggest that, with a few possible exceptions involving highly specialized neurons, all synapses contain synapsin I. Finally, immunocytochemical experiments indicate that synapsin I appearance in the various regions of the developing nervous system correlates topographically and temporally with the appearance of synapses.

In two accompanying papers (De Camilli, P., S. M. Harris, Jr., W. B. Huttner, and P. Greengard, and Huttner, W. B., W. Schiebler, P. Greengard, and P. De Camilli, 1983, *J. Cell Biol.* 96:1355–1373 and 1374–1388, respectively), evidence is presented that synapsin I is specifically associated with synaptic vesicles in nerve endings.

Synapsin I (formerly referred to as protein I) is the collective name for two peptides, synapsin Ia and synapsin Ib (protein Ia and protein Ib) with very similar properties. It was discovered as a major endogenous substrate for cAMP-dependent phosphorylation in mammalian brain (26, 50). Later studies showed that synapsin I is also a major endogenous substrate for Ca/calmodulin-dependent phosphorylation in brain (22, 23, 27, 28, 46). Synapsin I has been purified to homogeneity from

THE JOURNAL OF CELL BIOLOGY · VOLUME 96 MAY 1983 1337–1354

bovine brain (50; and footnote 1) and rat brain (22; and footnote 1), and extensively characterized. Synapsin I is an elongated protein, with a globular "head" and a proline-rich, collagenase-sensitive "tail" (50). Studies in living cells have shown that the state of phosphorylation of synapsin I is regulated by neurotransmitters and by depolarizing agents (12, 14, 36).

Synapsin I is present in mammalian brain at high concentrations (18, 24; and footnote 1). Previous immunochemical (11), immunohistochemical (4, 11), and subcellular fractionation (51) studies indicated that it is a neuron-specific protein, widely distributed in the central and peripheral nervous system, and concentrated at synapses. In the earlier immunohistochemical studies (4, 11), only a portion of synapses could be demonstrated to be immunoreactive. A major problem left open, therefore, was to determine the proportion of synapses that contain synapsin I and, if only some do, to determine which types of synapses contain it. To solve this problem, we have reanalyzed in detail the distribution of synapsin I in the adult nervous system of the rat. Our results indicate that synapsin I is present at the great majority of synapses and suggest that it may be present at all synapses, with the possible exception of some synapses involving highly specialized neurons. We have also carried out a preliminary analysis of the distribution of Synapsin I in developing nervous systems. The results indicate that synapsin I appearance in the nervous system parallels the appearance of synapses. A preliminary report of this work was presented in abstract form (9).

MATERIALS AND METHODS

Sprague-Dawley rats were obtained from Charles River Laboratories (Wilmington, MA), female New Zealand rabbits (weighing ~3.5 kg) from Pineacres (West Brattleboro, VT), chick specific pathogen-free avian supply embryos and adult chickens from specific pathogen-free avian supply (SPAFAS) (Norwich, CT). Glutaraldehyde, paraformaldehyde, and the components of Epon (Epon 812, dodecyl succinic anhydride (DDSA), nonenyl succinic anhydride (NMA), and 2,4,6-Tris-(dimethylaminomethyl)-phenol(DMP-30) were from Electron Microscopic Sciences (Fort Washington, PA); cyanogen bromide (CNBr)-activated Sepharose 4B was from Pharmacia (Uppsala, Sweden), complete Freund's adjuvant from Calbiochem-Behring Corp. (LaJolla, CA), 2-methylbutane from Eastman (Rochester, NY), bovine serum albumin (fraction V) from Sigma Chemical Co. (St. Louis, MO), gelatin from Fisher Scientific Co. (Pittsburgh, PA). Rhodamine-conjugated goat anti-rabbit IgG (heavy and light chains specific) was from Cappel Laboratories, Inc. (Cochranville, PA). Normal goat serum was obtained from a local farm.

Purification of Synapsin I

Synapsin I used for immunization of rabbits was purified from bovine brain. The purification procedure consisted of (*a*) preparation by conventional protein purification techniques of a fraction ("step V synapsin I") highly enriched in synapsin I (50), followed by (*b*) electrophoretic purification of this fraction to yield apparently homogeneous synapsin I ("pure synapsin I").

PREPARATION OF A FRACTION HIGHLY ENRICHED IN SYNAPSIN I ("STEP V SYNAPSIN I"): This fraction was prepared essentially as described by Ueda and Greengard (50) with the exception that a crude brain fraction was used instead of an M-1 preparation as the starting material for the extraction of synapsin I. This resulted in a much higher yield of synapsin I in the step V fraction. All operations were carried out at 4°C. Briefly, calf cerebral cortices (~1 kg) were homogenized in 4 vol of 0.32 M sucrose for 30 s in a Waring blender with a 2-min interval on ice after the first 15 s of homogenization. The homogenate was then mixed with an equal volume of 0.32 M sucrose and centrifuged at 10,000 *g* for 20 min in a Sorvall RC2-B centrifuge (DuPont Co., Newtown, CT) using a GSA rotor. The pellet thus obtained was suspended in ~1 l of 5 mM sodium phosphate buffer. The resulting suspension was then processed as indicated for steps 2–5 of reference 50.

ELECTROPHORETIC PURIFICATION: This step was preceded by partial phosphorylation of the "step V synapsin I" (50), to facilitate localization of synapsin I in gels. 1.6 ml of partially phosphorylated "step V synapsin I" (containing ~1 mg of synapsin I) in "SDS-stop solution" was loaded on a 7% SDS polyacrylamide gel (separating gel dimensions, 17 × 40 × 0.2 cm) and subjected to electrophoresis as described (50). The stacking gel (4.5% polyacrylamide, 3.5 cm long) had been polymerized without a slot-forming comb. Electrophoresis was carried out until synapsin I had reached the bottom portion of the gel. These electrophoretic conditions allowed adequate separation of synapsin I from two faster migrating phosphoproteins. The wet gel was then wrapped in Saran wrap and autoradiographed. Subsequently, the synapsin I-containing region of the gel was excised using the position of phospho-synapsin I in the autoradiograph as a guide. Synapsin I was eluted electrophoretically from the gel piece into a dialysis bag, using the buffer system employed in the previous electrophoresis step. A portable β-counter (Eberline Instrument Co., Ledyard, CT) was used to monitor the transfer of synapsin I from the gel piece to the dialysis bag. When elution appeared to be complete, the material that had accumulated in the bottom part of the dialysis tube, and which contained all the radioactivity, was carefully collected. The bulk of the SDS in this material was removed by cooling the sample to 4°C during centrifugation for 30 min at 3,000 *g* in an International centrifuge (International Equipment Co., Damon Corp., Needham Heights, MA). Under these conditions, a large pellet of SDS precipitate was formed. The supernatant that contained the synapsin I is referred to as "pure synapsin I." The concentration of synapsin I in this fraction was determined by the method of Lowry et al. (30) (using bovine serum albumin as a standard[2]) on aliquots concentrated as described in reference 16 by sequential TCA and acidified acetone precipitation. Other aliquots of "pure synapsin I" were subjected to SDS PAGE (Fig. 1) to confirm the purity of the synapsin I. ~600–700 μg of purified synapsin I was obtained from each preparative gel (~60–70% recovery of the synapsin I loaded on the gels). The "pure synapsin I" was used as the immunogen. In some cases, synapsin Ia and synapsin Ib were eluted separately from the gel.

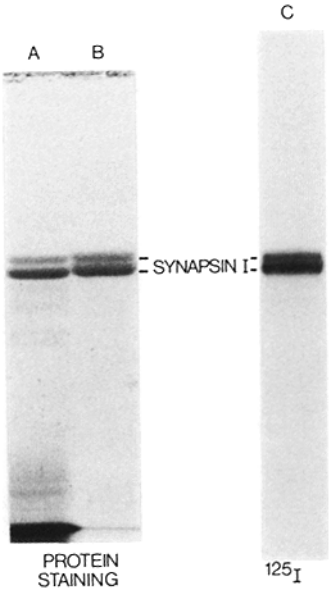

FIGURE 1 Purity of the synapsin I preparation used to raise antisera, and specificity of one such antiserum. *Left:* Coomassie Blue-stained 8% SDS polyacrylamide gel. The two lanes show the protein staining patterns of 90 μg of "step V synapsin I" (*A*) and of 6 μg of "pure synapsin I" (*B*). The slightly slower mobility of the synapsin I doublet in B is due to the partially phosphorylated state of synapsin I. *Right:* Autoradiograph of an 8% SDS polyacrylamide gel after radioimmunolabeling for synapsin I by the antibody-^{125}I-Protein A technique. 200 μg of total rat brain homogenate was used in this experiment.

Immunization of Rabbits

Two rabbits were immunized. The rabbits were bled 1 wk before immunization to obtain preimmune serum. Each rabbit received three successive injections of 200 μg of "pure synapsin I" at 2-wk intervals. Each administration consisted of a 2.5-ml suspension of synapsin I in complete Freund's adjuvant (1 vol of synapsin I in buffer, 1.5 vol of adjuvant), which was injected intradermally at multiple sites. Collection of antisera started 2 wk after the last injection.

Characterization of Antisera

SDS polyacrylamide gels of total homogenates of rat and bovine tissues and nonequilibrium pH gradient electrophoresis (NEPHGE) polyacrylamide gels (37) of crude synaptosomal fractions were prepared as described in references 11 and 23, respectively. Radioimmunolabeling of these gels was performed as described (11).

Double immunodiffusion tests were performed in a 2% agarose matrix prepared in a barbital-glycine/Tris buffer (pH 8.8) (ionic strength 0.08) (53), which also contained 0.1 M NaCl and 1% Triton X-100.

[1] DeGennaro, L. J., and P. Greengard. Manuscript in preparation.

[2] Synapsin I and bovine serum albumin give essentially identical specific colorimetric readings when assayed by the method of Lowry (Louis J. DeGennaro, personal communication).

Immunohistochemical Procedures

FIXATION AND TISSUE PREPARATION: Rats and adult chickens were anesthetized by ether. All animals were transcardially perfused at a pressure of 120 mm of Hg for 5 min with ice-cold 120 mM sodium phosphate buffer (pH 7.4) and then for 10–15 min with fixative in the same buffer. 4% (wt/vol) formaldehyde or 3% (wt/vol) formaldehyde plus 0.25% (wt/vol) glutaraldehyde was used as the fixative. Formaldehyde was always freshly prepared from paraformaldehyde just before use (17). Brains and other organs of interest were subsequently removed and immersed in the same fixative used for the perfusion for an additional 3 h at 0°C. Brains were cut into 1–2 mm thick coronal or sagittal slabs before this step. At the end of the 3 h, excess fixative was removed by several changes of 0.12 M sodium phosphate buffer.

Tissue specimens to be used for frozen sections were then infiltrated with sucrose by passing them through a series of increasing concentrations of sucrose (up to 18%, wt/vol) in 0.12 M sodium phosphate buffer, and stored in 0.12 M sodium phosphate buffer, 18% (wt/vol) sucrose, and 0.03% (wt/vol) NaN_3.

Tissue specimens to be used for plastic sections were dehydrated in graded ethanols and propylene oxide and embedded in Epon (17, 31).

All micrographs shown in the present paper were obtained from tissues fixed with 4% formaldehyde alone, except for Figs. 5 *b* and 12 *a*.

PREPARATION OF FROZEN AND PLASTIC SECTIONS: To prepare frozen sections, tissue slabs were frozen by immersion in isopentane chilled with liquid nitrogen, equilibrated in a cryostat (IEC Minotome) at −25°C, and sectioned serially at a thickness of 10–20 μm. Sections were then mounted on glass microscope slides and briefly air-dried. To obtain a good adhesion of the sections to the glass slides, the latter were pretreated by a brief immersion in a solution containing 1.5% (wt/vol) gelatin, 30% (vol/vol) ethanol, 0.1% (wt/vol) chromium potassium sulfate and 7% (vol/vol) acetic acid, followed by air-drying.

For plastic sections, Epon-embedded tissue blocks were cut at a thickness of ~1 μm on an ultracut microtome (Reichert, Wien, Austria), and the sections were collected on glass microscope slides pretreated as described for the frozen sections. Epon was removed as described by Maxwell (33). Briefly, 2 gm of KOH in pellets were added to 10 ml absolute methyl alcohol and 5 ml propylene oxide. The mixture was stirred for ~5 min until the KOH pellets had disintegrated. The mixture was then overlaid at room temperature on the plastic sections and allowed to act for ~2–5 min. Finally, sections were thoroughly rinsed with methanol and then with water using the stream from a wash bottle. The time necessary to completely remove the Epon from the 1-μm-thick sections was found to vary slightly depending upon the relative proportions of DDSA and NMA in the Epon mixture.

IMMUNOSTAINING: For immunostaining, the frozen sections, and the plastic sections after removal of the Epon, were processed in sequence through the following steps, at room temperature except where indicated. Step 1: incubation for 30 min in the presence of 0.1 M glycine buffered at pH 7.4 with Tris base; step 2: incubation for 3 h at 37°C with rabbit preimmune serum or rabbit anti-synapsin I antiserum diluted (1:50–1:100) in Triton buffer (0.3% [wt/vol] Triton X-100, 0.45 M NaCl, 0.02 M sodium phosphate buffer, pH 7.4) which also contained normal goat serum (i.e., nonimmune serum from the same animal species from which the second antibody was obtained) diluted 1:6; step 3: 30-min wash in Triton buffer; step 4: incubation for 1 h at 37°C with rhodamine-conjugated goat IgGs directed against rabbit IgGs (the goat IgGs were diluted in Triton buffer containing normal goat serum diluted 1:6); step 5: 30-min wash in Triton buffer; step 6: final rinse in 5 mM sodium phosphate buffer (pH 7.4). When tissues had been fixed by the formaldehyde-glutaraldehyde fixative solution, the immunostaining procedure described above was preceded by overlaying sections for 10 min with a freshly prepared solution of 1% Na borohydride in H_2O, in order to quench unreacted aldehyde groups of glutaraldehyde; sections were then rinsed with H_2O and processed starting with step 2. Antibody incubations were performed by overlaying each section with ~30–50 μl of antibody-containing solution that had been spun for 4 min in an Eppendorf microfuge (model 5412; Brinkmann Instruments, Inc., Westbury, NY) to remove aggregates. Washes were performed by several rinses with a stream from a wash bottle.

Nonspecific fluorescence of nuclei was sometimes observed after immunostaining of plastic sections, especially when tissues had been fixed by formaldehyde alone (see Figs. 4 and 7). This nonspecific staining was more prominent on nuclei with condensed chromatin. It could be reduced or abolished by using primary antisera at higher dilutions and increasing the temperature at which sections were incubated with antibodies (nuclear staining was maximum at 0°C, minimum at 37°C).

MICROSCOPY AND PHOTOGRAPHY: At the end of the immunostaining, the glass slides were mounted with 95% (vol/vol) glycerol/12 mM sodium phosphate buffer (pH 7.4) and examined in a Zeiss universal photomicroscope II equipped with epifluorescence optics and with oil-immersion Plan Neofluar (16× and 25×) and Planapo (40× and 63×) objectives. Photographs were taken using Kodak Plus-X-Pan film (except the micrograph shown in Fig. 3 *b* which was taken with Kodak Tri-X-Pan film), which were then developed using Kodak D76 diluted 1:1.

Due to differences in experimental conditions and in exposure times at the microscope and in the printing process, differences in the brightness of fluorescence staining among micrographs shown in this paper do not represent actual differences in immunoreactivity except when indicated.

Gel Electrophoresis

Electrophoresis in SDS polyacrylamide gels was performed as described (50).

Protein Determination

Protein was assayed by the method of Lowry et al. (30).

RESULTS

Preparation and Characterization of Rabbit Antisera Directed against Synapsin I

Synapsin I used as the immunogen was purified by a procedure involving SDS PAGE as the final step. The protein profiles of the fraction subjected to the final purification step (step V synapsin I) and the final fraction (pure synapsin I) are shown in Fig. 1. In the step V synapsin I, no major protein staining bands were visible in the gel in the immediate vicinity of synapsin I. However, this fraction contained, in addition to synapsin I, a large amount of very low molecular weight peptides, which are responsible for the dark band at the front of the gel shown in Fig. 1 *A*, as well as some minor bands with electrophoretic mobilities slightly faster than synapsin I. Most of the contaminating peptides were found to be phosphoproteins and appeared primarily to be proteolytic fragments of synapsin I. All of the observable contaminating peptides were readily separated from synapsin I in the long preparative gels used for the last purification step as seen from the protein profile of "pure synapsin I" (Fig. 1 *B*).

"Pure synapsin I" was injected into two rabbits. Experiments carried out with an antiserum prepared previously to native

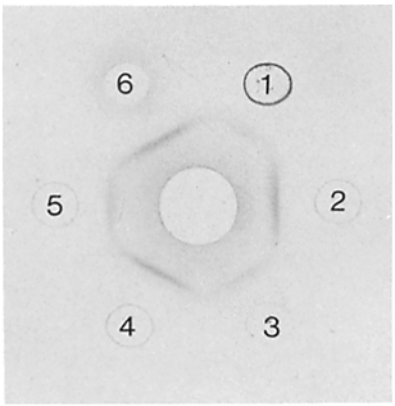

FIGURE 2 Coomassie Blue-staining of an agar double-immunodiffusion plate. 8 μl of antiserum (11) directed against synapsin I were applied to the central well. Additions (3 μl each) to the peripheral wells were as follows: *1* and *2*, 0.6 μg of pure synapsin I (synapsin Ia + synapsin Ib). (Excess SDS had not been removed from sample *1*, possibly accounting for the weaker precipitation line.) *3* and *5*, 0.13 μg of synapsin Ia; *4*, 0.4 μg of synapsin Ib; *6*, 0.6 μg of native synapsin I (synapsin Ia + synapsin Ib) purified as described in reference 50. The almost complete fusion of precipitation lines formed by the antiserum with synapsin Ia, synapsin Ib, and the synapsin I doublet indicates that the great majority of antigenic determinants are identical in synapsin Ia and synapsin Ib.

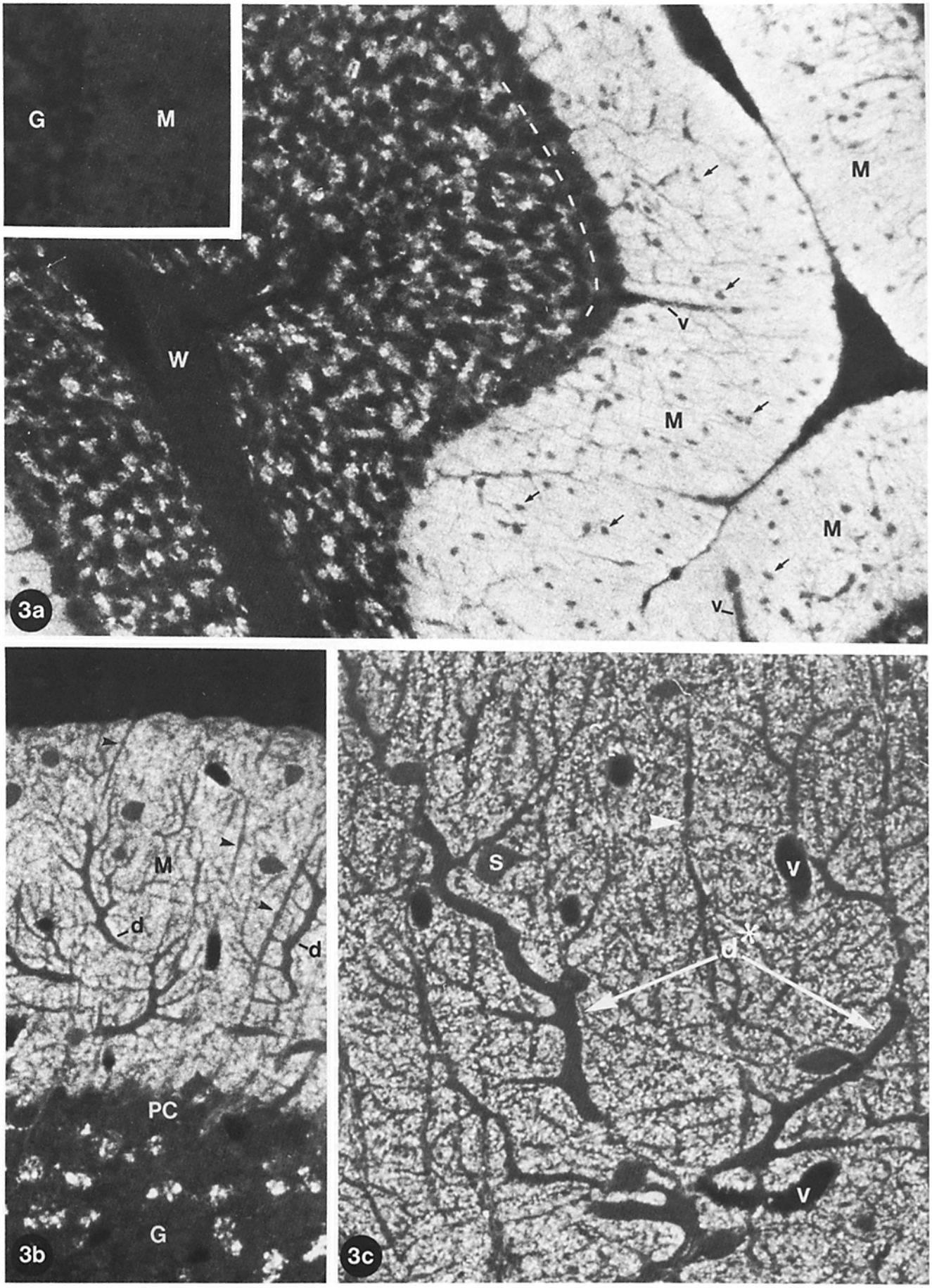
G
M
W
M
v
M
M
v
3a
M
d
d
PC
G
3b
S
v
v
3c

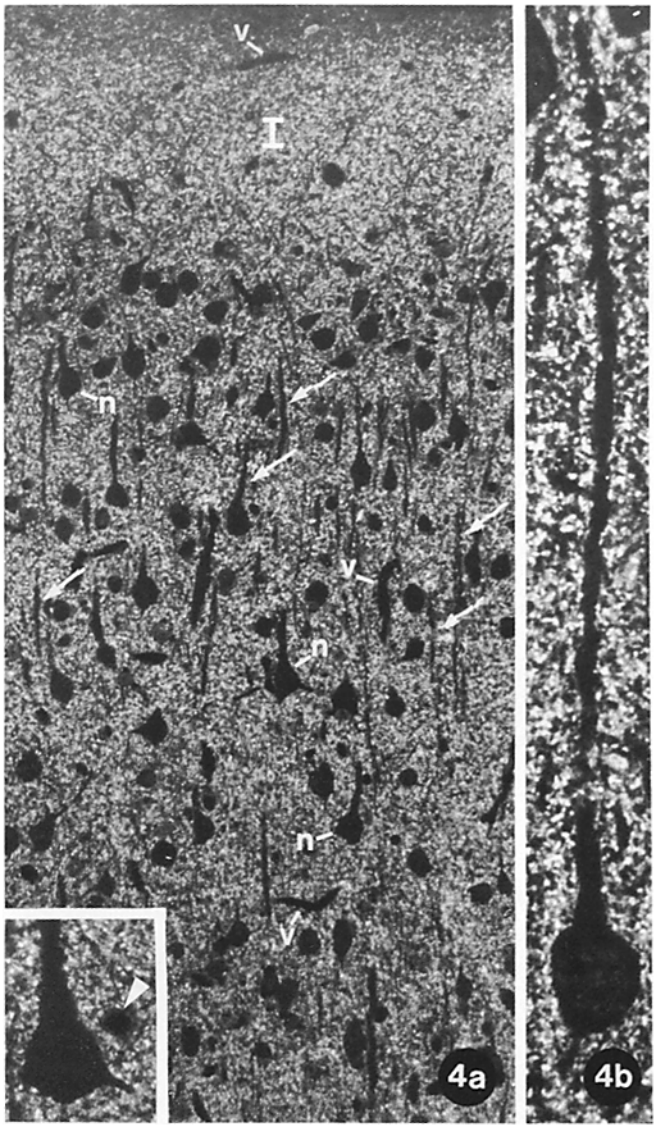

FIGURE 4 Fluorescence micrograph illustrating the distribution of Synapsin I immunoreactivity in rat cerebral cortex 0.1-μm-thick plastic sections. (*a*) Tightly packed, brightly fluorescent dots are visible in the neuropile throughout the field. Dark, nonfluorescent images are neuron cell bodies (*n*), major dendrites, and blood vessels (*v*). Particularly prominent are the negative images of the pyramidal cell apical dendrites (arrows) which run in parallel bundles toward layer I (*I*), where they branch. *Inset:* An enlargement of the negative image of the cell body of a pyramidal cell is shown. The emergence of the large apical dendrite and of a smaller basal dendrite are visible. The dark image indicated by an arrowhead is a capillary, which is recognizable by the presence of low-level nonspecific fluorescence on the C-shaped nucleus of the endothelial cell. (*b*) Section cut parallel to the orientation of a pyramidal cell apical dendrite, so that the dendrite is visible for a large portion of its length. Note the resolution of individual synapses and their heterogeneous size and brightness. The weak fluorescence of the nucleus of the pyramidal cell is of nonspecific nature. *a*, × 224; *inset*, × 720. *b*, × 1,000.

synapsin I (11) showed that synapsin Ia and Ib shared a great majority of their antigenic determinants (Fig. 2). Therefore, in preparing new antisera to be used in this study, we injected the synapsin I doublet. Both animals produced antisera that specifically recognized synapsin I when tested against peptides of total bovine or rat brain homogenates separated in an SDS polyacrylamide gel (Fig. 1). Neither one of the two antisera recognized proteins IIIa and IIIb, two related neuronal phosphoproteins (5, 21). We also used one of the two antisera to radioimmunolabel the peptides contained in a crude synaptosomal fraction after their separation in a NEPHGE gel (23, 37). In this NEPHGE gel, polypeptide bands co-migrating with synapsin I (23) were the only labeled bands (not shown). These results argue against the possibility that a minor contaminating immunogenic peptide was present in the step V synapsin I and co-migrated with synapsin Ia or Ib in the SDS polyacrylamide gel system used for the final purification of synapsin I.

All results reported in this paper (except for Fig. 2) and in the two accompanying papers (10, 24) were obtained by using one or the other of these two antisera. The two antisera gave results which were indistinguishable. These results, in turn, were identical to those obtained when the antiserum previously raised against native synapsin I (11) was used.

Distribution of Synapsin I Immunoreactivity in the Central Nervous System

When the antiserum directed against synapsin I was used to stain frozen and plastic sections by immunofluorescence, a bright fluorescence was observed in the neuropile of all regions of the central nervous system examined, which included the retina, the spinal cord and all the major brain regions. This fluorescence was dependent on the presence of antibodies

FIGURE 3 Distribution of synapsin I immunoreactivity in rat cerebellar cortex as revealed by immunofluorescence in sagittal sections. In this and in the following pictures immunoreactive material appears white. (*a*) 10-μm-thick frozen section. Bright fluorescence is present throughout the molecular layer of the three adjacent cortical folds visible in the field. Immunoreactivity in the molecular layer appears very diffuse. Dark, nonfluorescent regions are glial cells, neuronal perikarya (arrows), and blood vessels. One can also see the black meshwork of unstained dendrites, predominantly originating from Purkinje cells that line the molecular layer at its inner surface. A dotted line outlines the position of unstained perikarya of Purkinje cells. In the granule cell layer, synapsin I immunoreactivity has a patchy distribution that corresponds to the distribution of cerebellar glomeruli. Dark spaces among these patches correspond to the perikarya of the small granule cells. No fluorscence is visible in the white matter. *Inset:* 10-μm-thick frozen section processed by the same immunostaining procedure used for the main picture but in which rabbit preimmune serum replaced the rabbit anti-synapsin I antiserum. (*b* and *c*) 1-μm-thick plastic sections. All the layers of the cerebellar cortex are visible in *b*. A high magnification of the molecular layer is shown in *c*, where immunoreactivity in the neuropile is resolved into discrete dots that probably correspond to individual synapses. The substantially greater resolution of cellular detail in *c* than in *b* is also partially due to the different speed of the film used to obtain the two micrographs (see Materials and Methods). *M*, molecular layer; *PC*, Purkinje cell layer; *G*, granule cell layer; *W*, white matter; *d*, dendrites of Purkinje cells; *d**, dendrites originating from the same Purkinje cell; *v*, blood vessels; *s*, stellate cells. The long nonimmunoreactive processes extending from the Purkinje cell layer to the pial surface and oriented perpendicular to the pial surface (arrowheads) are probably Bergmann glial processes. *a*, × 244; *inset*, × 250. *b*, × 640. *c*, × 1,040.

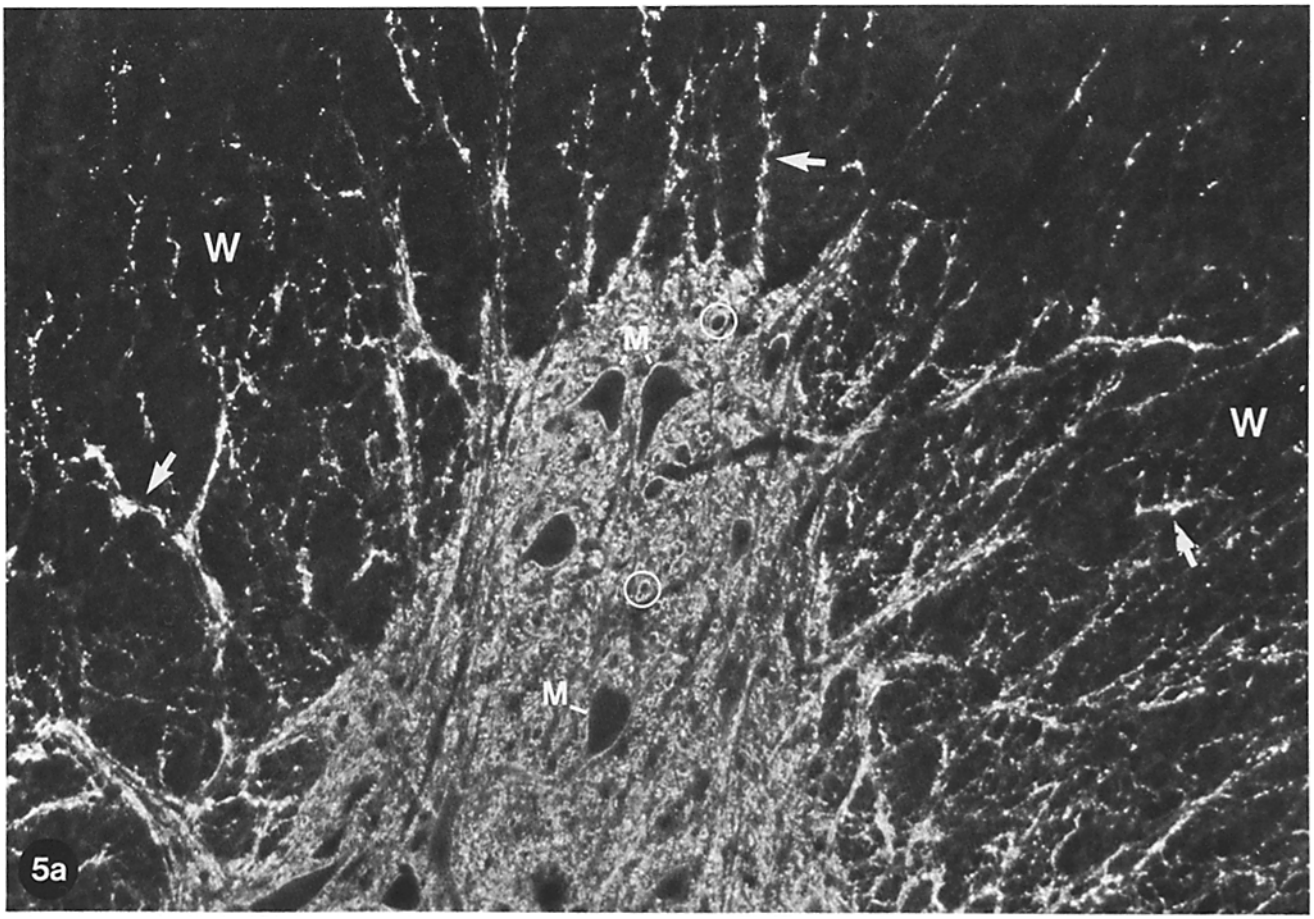
W
M
W
M
5a

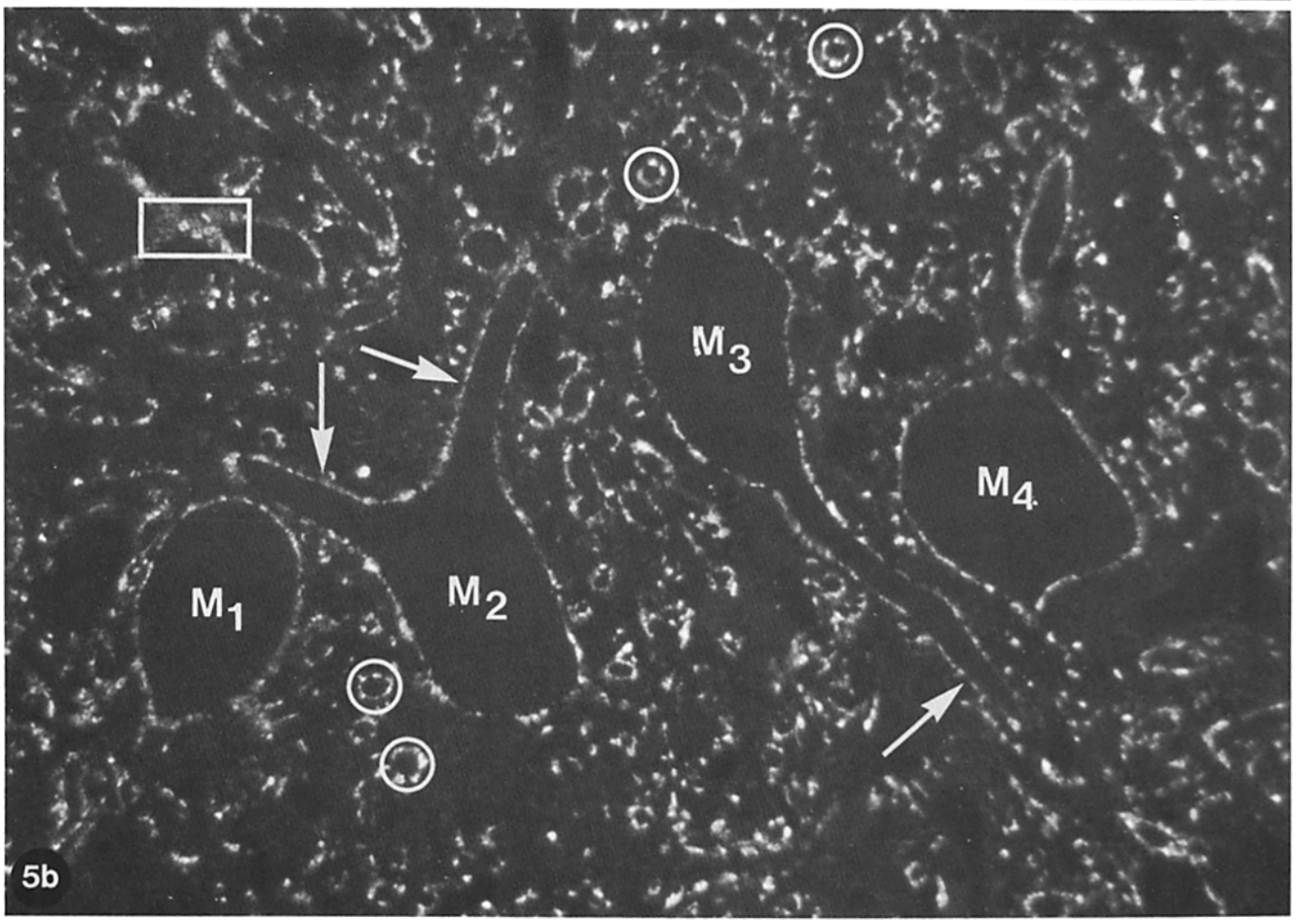
M3
M4
M1
M2
5b

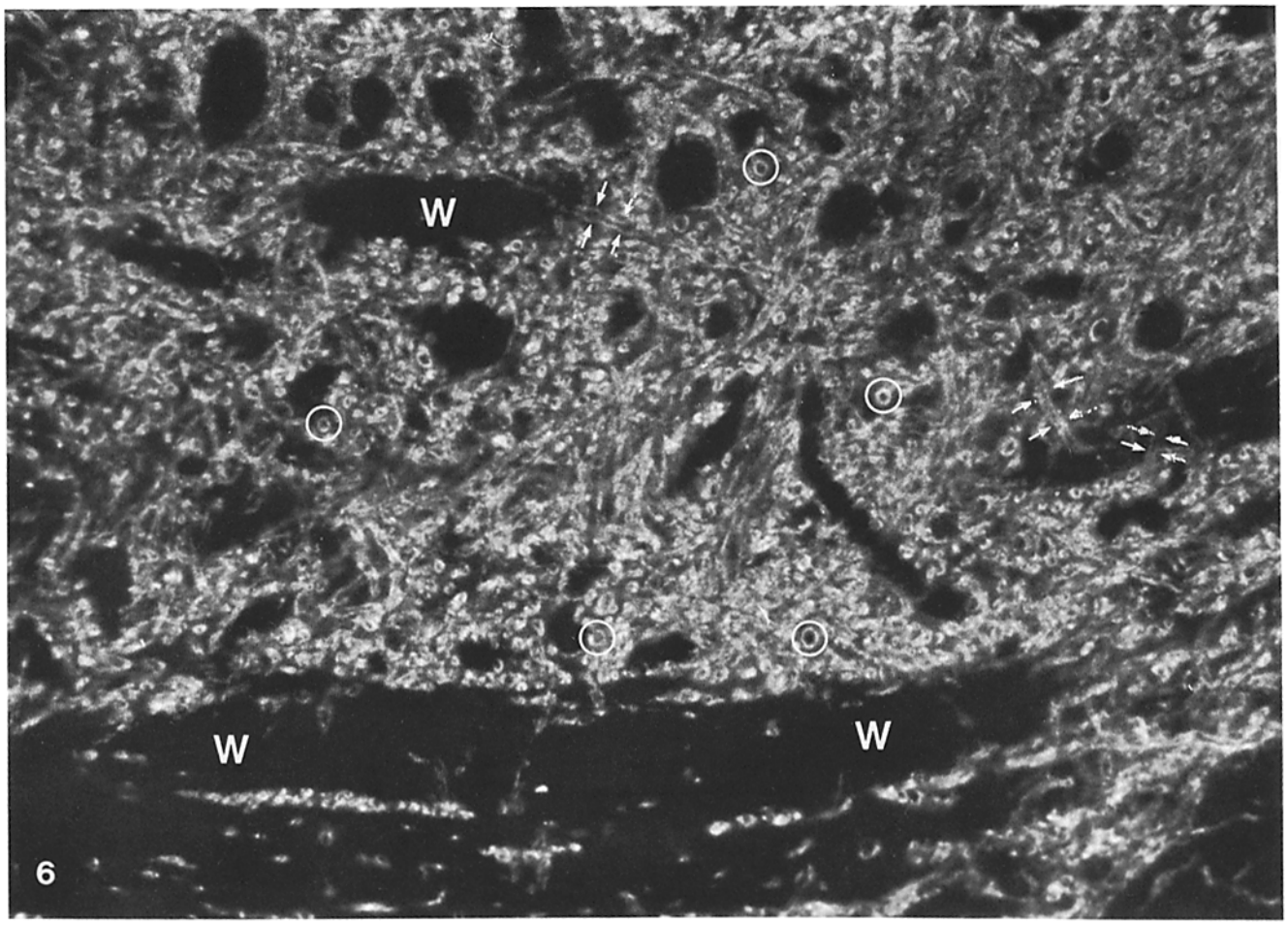

FIGURE 6 Fluorescence micrograph illustrating distribution of synapsin I immunoreactivity in the pars reticulata of the substantia nigra. 10-μm-thick frozen sagittal section. Immunoreactive material forms rings (white circles) or pairs of parallel lines (arrows). *W*, tracts of white matter of the crus cerebri. × 490.

directed against synapsin I in the rabbit serum, since only a weak fluorescence, almost indistinguishable from the autofluorescence of the tissue, was observed when rabbit preimmune serum was used. Several representative examples of sections immunostained with anti-synapsin I antibodies are shown in Figs. 3–6.

Fig. 3 *a* shows a frozen section of the cerebellum. As can be seen, fluorescence is present only in those regions that contain synapses. Thus, a patchy fluorescence is visible in the granule cell layer where synapses are clustered in glomeruli; in contrast, an almost continuous fluorescence is visible in the molecular layer where synapses are very abundant and rather homogeneously dispersed (38). (The inset of Fig. 3 *a* shows control staining of the cerebellum performed with preimmune serum and demonstrates that the immunofluorescence stain in synapses is of specific nature.) All glomeruli appear equally labeled and fluorescent intensity in the molecular layer appears uniform, i.e., without regional variations. Neuronal cell bodies, nonneuronal cells, and white matter are unstained. Dendrites visible in the molecular layer appear to be unstained but their negative images are rather blurred due to the considerable thickness (10 μm) of the frozen section. A much higher resolution of immunoreactive and nonimmunoreactive structures in the molecular layer was obtained when immunofluorescent staining for synapsin I was performed on Epon sections (1 μm thick) (Fig. 3 *b* and *c*). Synapsin I immunoreactivity was preserved in the plastic preparations, in spite of the protein denaturing step involved in Epon embedding and subsequent Epon removal. The negative "silhouettes" of unstained dendrites and of other unstained cellular processes (such as the radial processes of Bergmann glia [38]) are sharply outlined in plastic sections (Fig. 3 *b* and *c*). Furthermore, the fluorescent

FIGURE 5 Fluorescence micrograph illustrating distribution of synapsin I immunoreactivity in the anterior horn of the rat spinal cord. (*a*) 10-μm-thick frozen transverse section. Immunoreactivity is visible in the gray matter and in its radiations into the white matter (arrows), but not in the white matter (*W*). The dark images of unstained motor neuron cell bodies (*M*) and their dendrites are sharply outlined by rows of fluorescent synapses. (*b*) 1-μm-thick plastic transverse section. The profiles of the perikarya of four motor neurons (M_1–M_4) outlined by fluorescent synapses on their surfaces are visible. Arrows indicate dendrites emerging from M_2 and M_3. The white rectangle indicates a region where the section has been cut tangentially to the surface of a large dendrite so that synapses on this dendrite are seen en face. Cross sections of dendrites surrounded by fluorescent synapses are indicated by white circles in *a* and *b*. *a*, × 210. b, × 850.

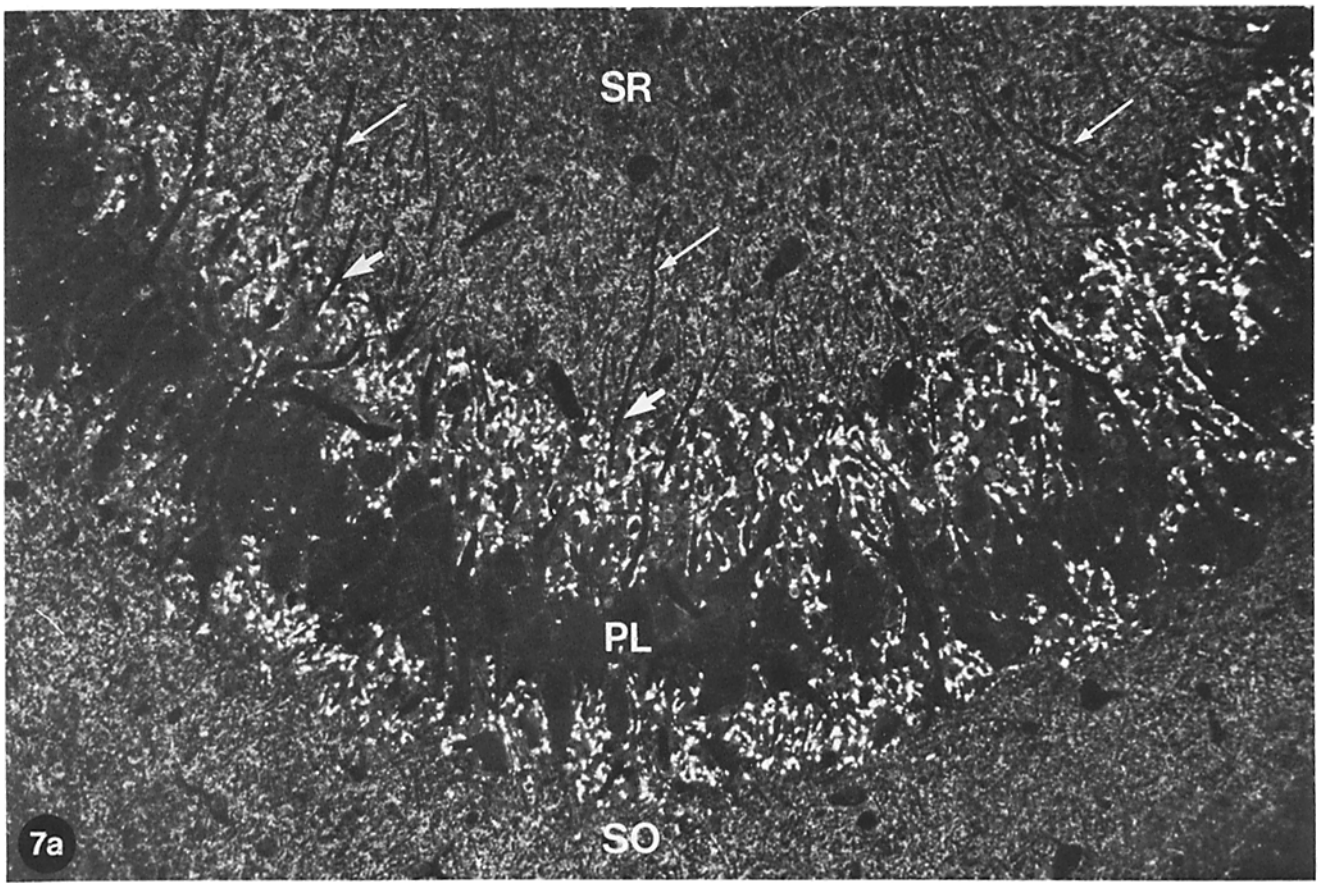
SR
PL
SO
7a

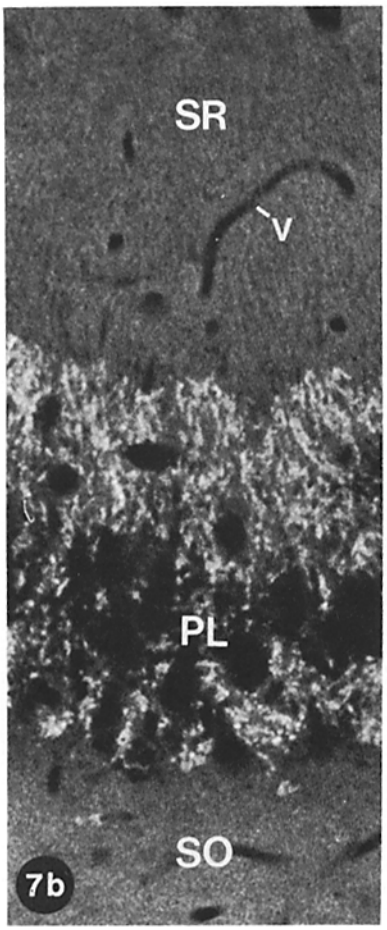
SR
V
PL
SO
7b

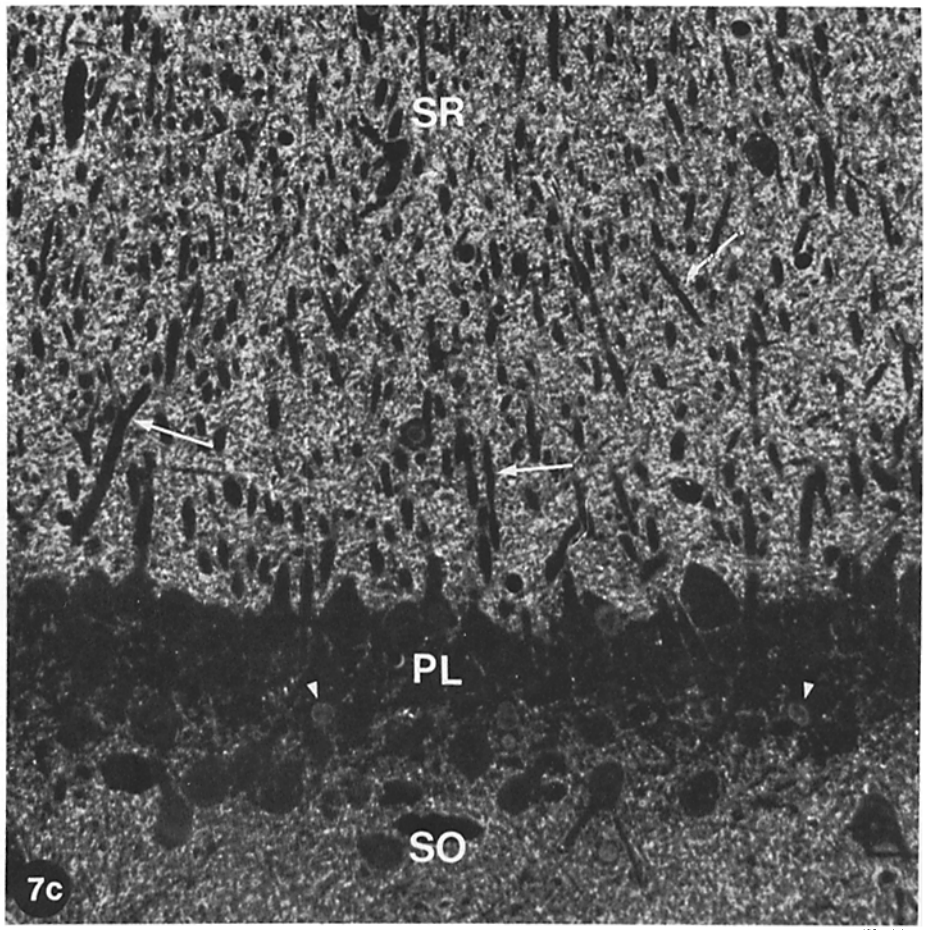
SR
PL
SO
7c

stain in the molecular layer, which had a grainy but rather diffuse appearance in frozen sections (Fig. 3 *a*), is clearly resolved into discrete dots in plastic sections when viewed at sufficiently high magnification (Fig. 3 *c*). The size and distribution of these dots is compatible with their being immunostained nerve endings (38).

Fig. 4 shows a plastic section of the cerebral cortex cut almost perpendicular to the pial surface. As in the molecular layer of the cerebellum, tightly apposed fluorescent dots are visible throughout the neuropile of the cerebral cortex, where synapses are densely packed. Neuronal perikarya, dendrites, and nonneuronal cells do not show any specific fluorescence. A similar staining pattern was observed throughout all regions of the cerebral cortex.

The close apposition of immunoreactive dots visible in plastic sections (Figs. 3 *c* and 4) in regions of gray matter very rich in synapses, such as the cerebral and cerebellar cortex, suggests that all nerve terminals may contain synapsin I. Thus, the thickness of plastic sections (~1 μm) is in the same size range as that of average axon terminals (41). This means that the tight packing of fluorescent dots visible in plastic sections cannot be explained by immunoreactive synapses located at variable depths within the section, but rather reflects closely the high density of distribution of immunoreactive synapses. The dark spaces visible in Figs. 3 *c* and 4 among fluorescent dots may be accounted for by the meshwork of axons and small dendrites and glial cell processes interspersed with nerve endings in the neuropile.

Fig. 5 shows immunostained frozen and plastic sections of the anterior horn of the spinal cord. Only the gray matter is stained (Fig. 5 *a*). In agreement with the abundance of axosomatic and axodendritic synapses on the motor neurons of the spinal cord (41), a large fraction of immunoreactive dots seems to be present on the surface of perikarya and dendrites of motor neurons. This is more evident in the plastic section shown in Fig. 5 *b*, where immunoreactive dots provide a sharp outline of neuronal cell bodies and of the major longitudinally sectioned and cross-sectioned dendrites. The fluorescent pattern is compatible with the possibility that most synapses contain synapsin I. As can be seen in Fig. 5 *b*, practically no space seems to be available on the surface of motor neurons to account for the presence of unstained synapses. The much lower density of immunoreactive dots per unit area in Fig. 5 *b* than in *a* is due to the different thickness of the two sections. This average density is also lower than that observed on plastic sections of the same thickness from the molecular layer of the cerebellum (Fig. 3 *c*) and from the cerebral cortex (Fig. 4). Thus, the fluorescent images obtained correlate with the lower density of synapses in the anterior horn of the spinal cord (6).

Fig. 6 shows an immunostained frozen section of the pars reticulata of the substantia nigra with the adjacent white matter of the crus cerebri. Immunofluorescent pairs of roughly parallel continuous lines, reminiscent of railroad tracks, and immunofluorescent rings, are the predominant features of the field. These "railroad track" and circular images can be explained by the synaptic architecture of this region. The synaptic meshwork in the pars reticulata of the substantia nigra is predominantly constituted by long, poorly ramified dendrites of the nigral neurons and by the axons that extensively innervate them (43, 45). Nerve endings on the surface of these dendrites form a regular and almost continuous sheath. Thus, synapses on longitudinally sectioned and cross-sectioned dendrites can account for the railroad track and circular fluorescence images, respectively. The continuity of the fluorescence profiles again suggests that all nerve endings contain synapsin I.

DISTINCT PATTERNS OF FLUORESCENT INTENSITIES IN SPECIFIC BRAIN REGIONS: As is clear from the immunostained plastic sections shown in Figs. 3 *c*, 4, and 5 *b*, the elementary unit of fluorescence stain of the neuropile, produced by antibodies directed against synapsin I, is a fluorescent dot that appears to correspond to an individual nerve terminal. Size and brightness of individual dots appeared to be somewhat variable but within a certain limited range. In a few regions of the brain, however, very large variations in size and brightness of individual dots were observed between adjacent portions of the neuropile. This, in turn, produced very distinct fluorescent patterns. Two examples are shown in Figs. 7 and 8.

Fig. 7 *a* and *b* shows the distribution of synapsin I immunoreactivity in plastic and frozen sections, respectively, of the CA_3 region of the hippocampus. A rather uniform distribution of very tiny immunoreactive dots is present throughout the gray matter of the strata radiatum and oriens. In contrast, in those portions of the neuropile close to the pyramidal cell perikarya, fluorescent dots are much larger, and are irregular in shape and very bright. These dots appear to line large dendrites and, in particular, the proximal portion of the large apical dendrites of pyramidal cells. A similar morphological distribution has been described for the mossy fiber terminals of axons that originate from the granule cells of the hippocampus (45, 48). These are very large nerve endings that establish multiple contacts with several postsynaptic elements, mostly with dendrites of pyramidal cells. It is, therefore, likely that the large bright fluorescent dots represent mossy fiber terminals. In support of this conclusion, these dots were not observed in the CA_1 region (Fig. 7 *c*), where mossy fiber terminals are not present (45, 48).

FIGURE 7 Fluorescence micrographs illustrating the distribution of synapsin I immunoreactivity in coronal sections of the rat hippocampus. *SR*, stratum radiatum; *PL*, pyramidal cell layer; *SO*, stratum oriens. (*a*) 1-μm-thick plastic section of the CA_3 region. Immunoreactivity is visible throughout the neuropile in the form of discrete dots. Cell bodies and dendrites are unstained. Particularly notable for their size and orientation are the negative images of apical dendrites of pyramidal cells (thin arrows). Immunoreactive dots are, in general, very small, except for the portions of the neuropile directly adjacent to the pyramidal cell layer, where the mossy fiber terminals are located. Here a band of large, brightly fluorescent dots is present at both sides of the pyramidal cell layer. These dots are more abundant at the apical side of pyramidal cells and seem to outline their dendrites. Thick arrows point to the transition from the proximal portion of dendrites lined by large dots to the distal portion of the same dendrites lined by small dots. (*b*) 10-μm-thick frozen section of the same region as in a, showing that the overall pattern of immunofluorescence is identical in plastic and frozen sections. *v*, Blood vessel. (*c*) 1-μm-thick plastic section of the CA_1 region of the hippocampus. A homogeneous punctate fluorescence is present in the neuropile. Cell bodies and dendrites are unstained. Arrows point to apical dendrites of pyramidal cells. Due to the orientation of the section, which is not exactly parallel to the direction of these dendrites, they are visible in the plane of the section only for a small portion of their length. The pale fluorescence visible on some cell nuclei (small arrowheads) is of nonspecific nature. *a*, × 490; *b*, × 490; *c*, × 420.

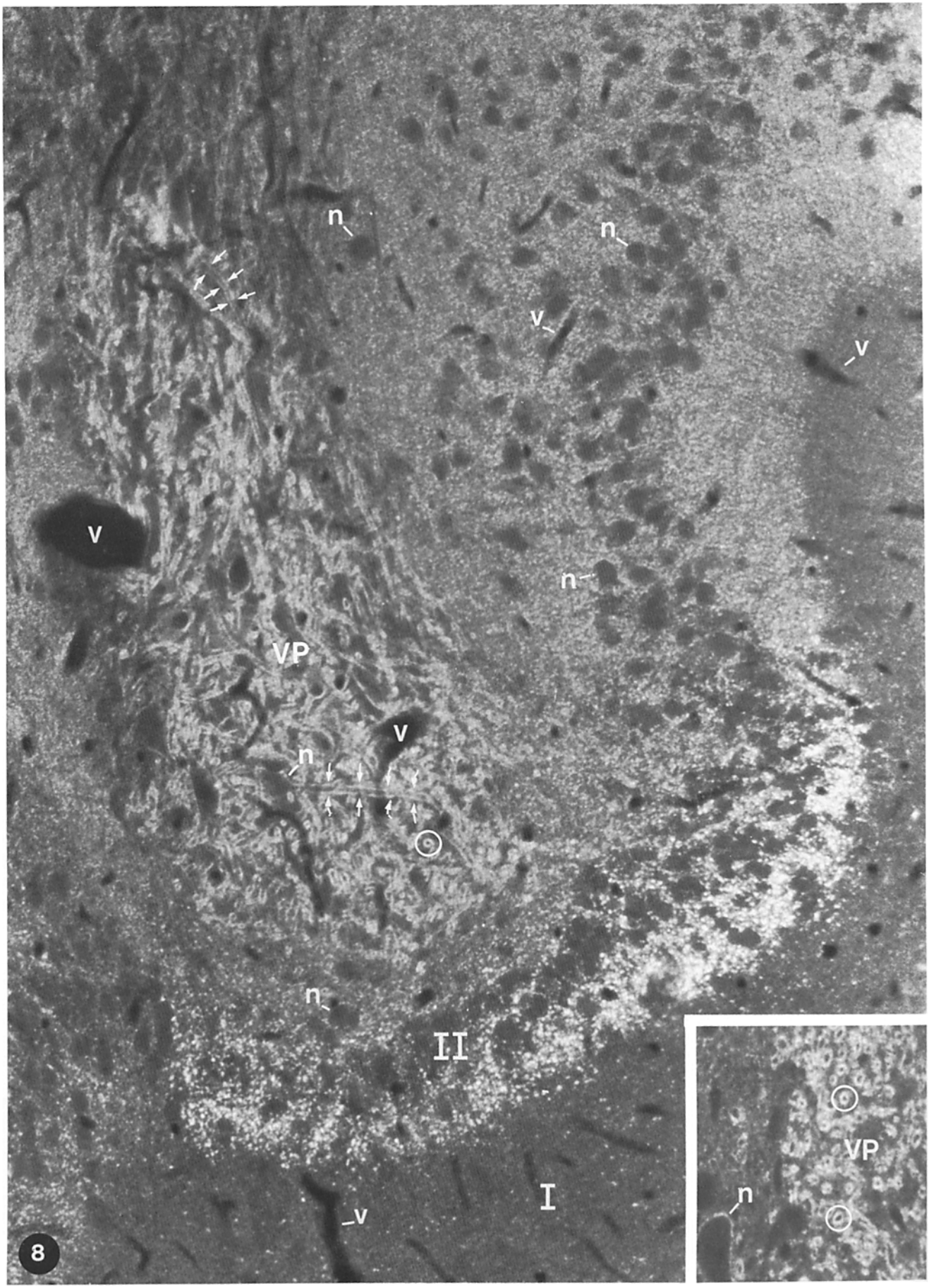
n
n
v
v
v
n
VP
v
n
n
II
I
v
8
VP
n

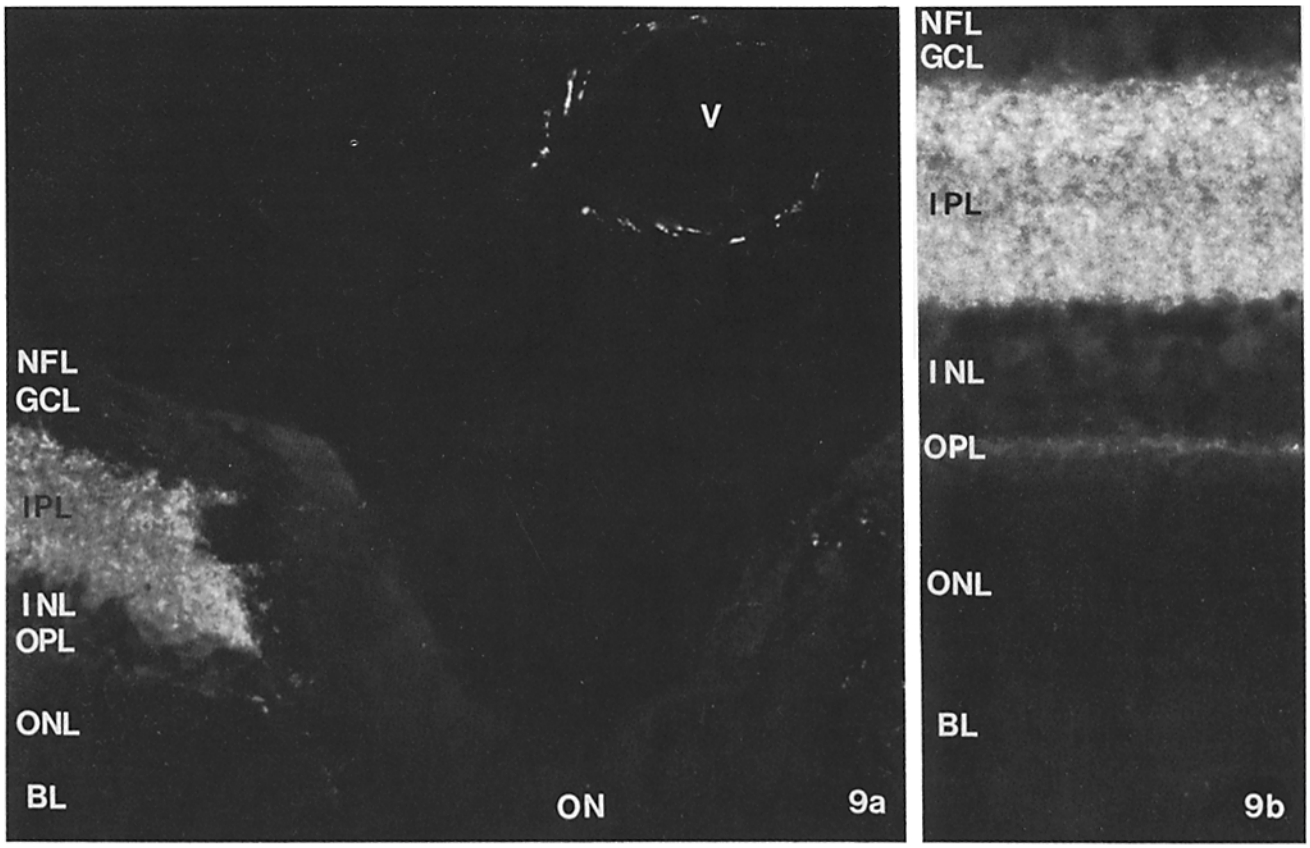

FIGURE 9 Fluorescence micrograph illustrating distribution of synapsin I immunoreactivity in the rat retina. 10-μm-thick frozen sections. *NFL*, nerve fiber layer; *GCL*, ganglion cell layer; *IPL*, inner plexiform layer; *INL*, inner nuclear layer; *OPL*, outer plexiform layer; *ONL*, outer nuclear layer; *BL*, bacillary layer (inner and outer segments of rods and cones). (*a*) The micrograph includes a portion of the optic papilla. A pale nonspecific fluorescence allows identification of axons of the nerve fiber layer that converge to form the optic nerve (*ON*). A blood vessel (*v*) surrounded by immunoreactive varicose terminals is visible in the vitreal space. (*b*) Section through the retina cut approximately halfway between the ora serrata and the optic nerve papilla. In both *a* and *b* the inner plexiform layer appears brightly fluorescent. Some discrete dots of immunofluorescence are also visible in the outer plexiform layer. *a*, × 352. *b*, × 600.

Fig. 8 shows a frozen section of the olfactory tubercle, which includes a fingerlike extension of the globus pallidus in this cortical region (ventral pallidum, see references 19, 20, 52). The texture of the fluorescent stain shows striking regional variations. In the central portion of the picture (ventral pallidum), synapsin I immunoreactivity is observed predominantly in a railroad track pattern, i.e., as pairs of parallel lines. This pattern is reminiscent of the pattern observed in the pars reticulata of the substantia nigra (Fig. 6), and in the main portion of the globus pallidus (not shown). In fact, these three regions are characterized by a similar synaptic architecture (20, 40, 43, 45). Around this central region of Fig. 8 and throughout most of the field, immunoreactive material appears rather uniformly dispersed throughout the neuropile, as in the majority of brain regions. Individual grains are poorly resolved, as is usually the case in frozen sections, but a band of larger and very bright spots is visible. On the basis of observations made in the hippocampus it seems likely that these immunofluorescent dots represent large nerve endings. However, there is a paucity of information concerning the ultrastructure of the neuropile in this region, and this interpretation will need to be tested by future studies.

RETINA: As in all other regions of the central nervous system containing synapses, both the outer and inner plexiform

FIGURE 8 Fluorescence micrograph illustrating distribution of synapsin I immunoreactivity in the rat ventral pallidum and olfactory tubercle. 10-μm-thick frozen sagittal sections. The main picture shows the distinct patterns produced by anti-synapsin I immunofluorescence in different neuropile regions. A grainy diffuse immunoreactivity is present throughout the gray matter. Variations, however, are apparent from region to region in the density and particularly in the size and brightness of immunoreactive dots. In the cortex of the olfactory tubercle a prominent band of large, bright fluorescent dots is visible at the apical side of the pyramidal cells of layer II at the region where this layer surrounds a fingerlike extension in the tubercle of the ventral pallidum (*VP*). In the ventral pallidum, immunoreactivity appears predominantly in the form of pairs of parallel lines (railroad track images) (arrows); these parallel lines correspond to axodendritic synapses, which form an almost continuous sheath on the dendrites of the ventral pallidum neurons (20). These dendrites are predominantly oriented in a caudo-rostral direction (in the micrograph from top to bottom) so that in coronal sections (*inset*) axodendritic synapses appear predominantly as fluorescent rings. *v*, Blood vessels; *n*, neuronal perikarya; *I* and *II*, layer I (molecular layer) and II (pyramidal cell layer) of the olfactory tubercle cortex; white circles enclose cross-sectioned dendrites. × 312; *inset*, × 512.

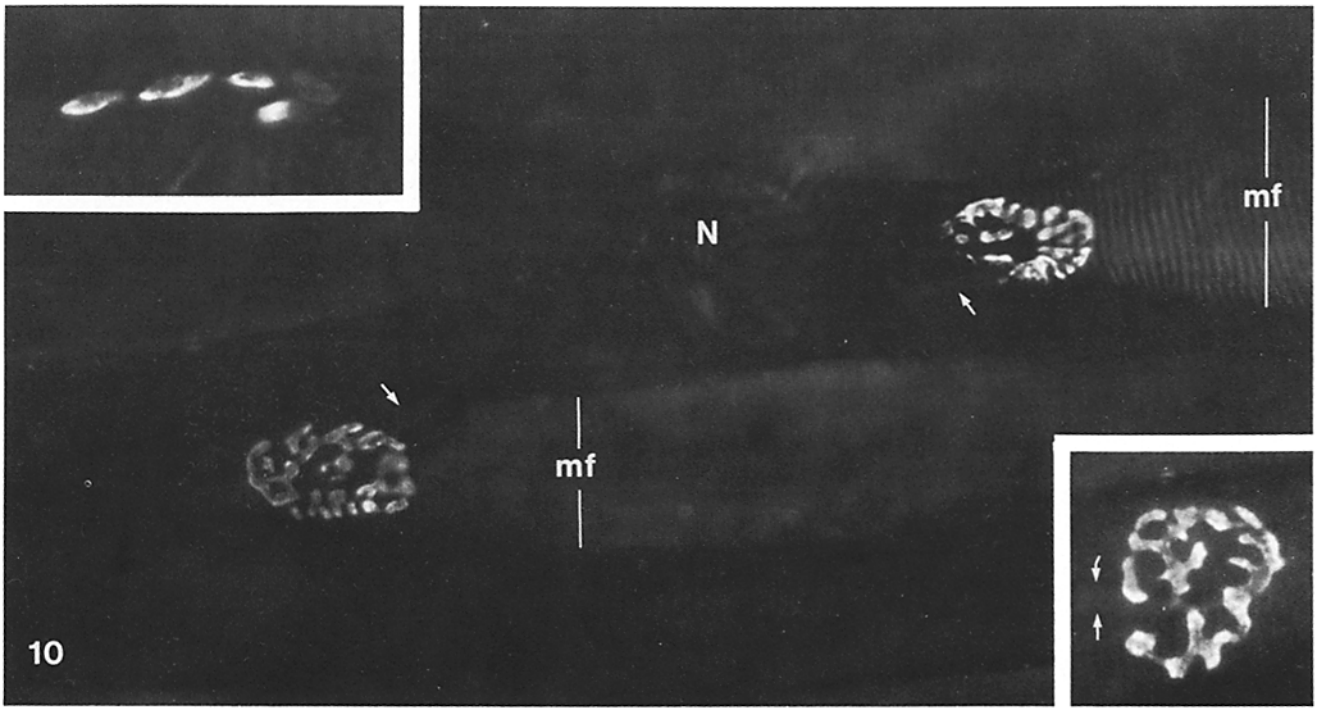

FIGURE 10 Fluorescence micrographs showing distribution of synapsin I immunoreactivity in the rat diaphragm. *Main field:* 20-μm-thick frozen section. En face view of two motor end plates. A low nonspecific fluorescence permits identification of the two axons (arrows) from which the two motor end plates originate and the branch of the phrenic nerve (*N*) from which these axons in turn derive. Striated muscle fibers (*mf*) are visible by their weak nonspecific fluorescence. *Bottom-right inset* (20-μm-thick frozen section): higher magnification of another motor end plate. Arrowheads indicate the axon that forms the junction. *Top-left inset:* 1-μm-thick plastic section. The field shows a cross section through some processes of a single motor end plate. Immunoreactivity appears to be concentrated only at one side of each process. × 573; *bottom-right inset*, × 742; *top-left inset*, × 1,120.

layers of the retina (42) showed synapsin I immunoreactivity (Fig. 9). The bright fluorescence in the inner plexiform layer was compatible with a localization of synapsin I in all synapses of this layer. Immunoreactivity in the outer plexiform layer, on the contrary, was not prominent and, in some experiments, even difficult to detect. A large fraction of terminals in the outer plexiform layer is constituted by photoreceptor cell terminals. Some of these (the cone pedicles [8, 44, 45]) are very large and should have been clearly detected if they contained synapsin I. Therefore, our findings leave open the possibility that photoreceptors, which are highly specialized neurons, might not contain synapsin I.

Distribution of Synapsin I Immunoreactivity in the Peripheral Nervous System

Synapsin I immunoreactivity appears to be present at all sites that contain nerve endings in the peripheral nervous system. Some examples are shown in Figs. 10–12.

Fig. 10 illustrates the presence of synapsin I immunoreactivity at the neuromuscular junction. The main picture and the bottom right inset show images obtained from thick (20 μm) frozen sections that allow visualization of the terminals of the motor end plate (7) throughout its entire depth. One can also see in these pictures the sharp transition from the nonimmunoreactive axon to the brightly fluorescent nerve ending. The top left inset shows a cross section of several processes of a single motor end plate from a plastic embedded specimen. One can also see, from both the frozen and plastic sections, that synapsin I immunoreactivity is not uniformly distributed within the nerve ending, but rather that it is highly concentrated in the regions closest to the synaptic cleft. This can be understood in terms of the large dimension of the synapse and nerve terminal at the neuromuscular junction.

Figs. 11 and 12 *a* and *b* show examples of nerve endings in the autonomic nervous system. Figs. 11 and 12 *a* show synapses in the sympathetic and parasympathetic ganglia (3), respectively. Fig. 12 *a* and *b* show en passant varicosities innervating peripheral tissues.

As in the central nervous system, synapsin I immunoreactivity was not detected in neuronal cell bodies in the peripheral nervous system (Figs. 11 and 12). Similarly, synapsin I immunoreactivity in general was not observed on axons (Figs. 10 and 11). Most nerve fibers including the major nerve trunks did not show any specific fluorescence when stained for synapsin I. However, at variance with this more general pattern, small dots or rods of immunoreactivity were often observed on the peripheral nerve fibers of the autonomic nervous system. Several examples are shown in Fig. 12 *c–f*. Size, shape, and brightness of these fluorescent spots were similar to those observed on en passant varicosities.

Appearance of Synapsin I during Ontogenesis

During ontogenesis, the appearance of immunohistochemically detectable synapsin I was found to correlate temporally and topographically with the appearance of synapses. We report here two examples of the distribution of synapsin I immunoreactivity, taken from the developing cerebella of the rat and the chick.[3] The development of the cerebellum in these two animal species is much different in that it occurs largely prenatally in the chick, whereas it is almost totally a postnatal

[3] Substantial cross-reactivity was observed between chick and rat synapsin I.

event in the rat (29). The architecture of the adult cerebellar cortex, however, is very similar in adults of the two species (29). Analogously, the distribution of synapsin I immunoreactivity was found to be similar in adults of the two species (not shown).

Fig. 13 shows frozen sections of the chick cerebellum at embryonic day 17. At this stage the major cellular elements characteristic of the adult cerebellum are already present. Many cells, however, have not yet reached their final positions and neuronal processes are still rudimentary (42). Only a few synaptic contacts have as yet developed (35, 42). Dots of synapsin I immunoreactivity decorate the primary dendrites of the poorly developed Purkinje cell dendritic tree. This localization of synapsin I immunoreactivity matches very closely previous descriptions of synaptogenetic events taking place at this stage of development of Purkinje cells in the chick cerebellum (35, 42). Only sparse dots of immunoreactivity are present in the granule cell layer where synapses are poorly developed (35).

Fig. 14 shows frozen sections of the rat cerebellum at postnatal day 9. At that time, the synaptic organization of the rat cerebellum is at a stage of development slightly more advanced than the chick cerebellum at embryonic day 17 (29, 42). Immunoreactivity is abundant in the very thin molecular layer, which is still surrounded by a prominent external granule layer. In the latter layer, no synapses are present (and correspondingly, no immunoreactivity is observed). Bright, but disperse, dots of immunoreactive material are present in the granule cell layer where glomeruli are still immature. Furthermore, immunoreactive dots are abundant around the perikarya of Purkinje cells, which at some regions are still arranged in multiple layers. Dots around Purkinje cell perikarya correspond to axosomatic synapses, which are very abundant on Purkinje cell bodies of the rat cerebellar cortex at this stage of development, but which will subsequently disappear (29, 42).

DISCUSSION

The present results confirm previous studies (4, 11) which had indicated that synapsin I (previously referred to as protein I) is a neuron-specific protein, highly concentrated at synapses. In addition, they clearly indicate that synapsin I has an even wider distribution throughout the nervous system than could be demonstrated in those preliminary studies. In frozen sections from a large number of regions of the central and peripheral nervous system, the distribution of synapsin I immunoreactivity appeared to match very closely the distribution and concentration of synapses. Furthermore, the high resolution images obtained in Epon sections have proven unambiguously that the uniform distribution of synapsin I immunoreactivity in the neuropile is due to the close apposition of immunoreactive synapses. In thick frozen sections, a uniform distribution of immunoreactivity might result from overlapping images of a minor proportion of immunoreactive synapses located at dif-

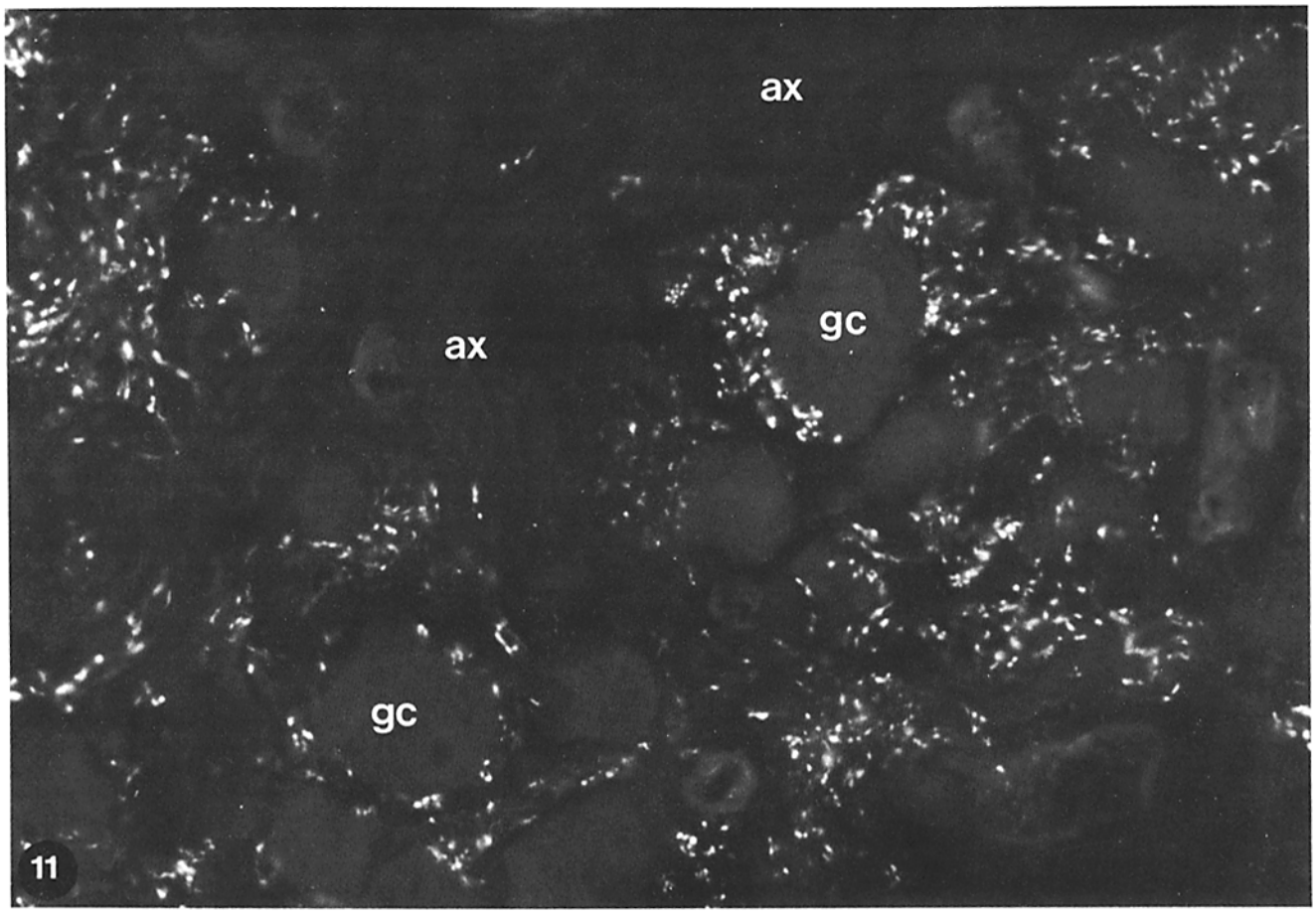

FIGURE 11 Fluorescence micrograph showing distribution of synapsin I immunoreactivity in the rat superior cervical ganglion. 10-μm-thick frozen section. Bright dots of immunoreactivity are interspersed among ganglion cells (*gc*) which are recognizable by a low-level, nonspecific fluorescence. The distribution of immunoreactive dots corresponds to the localization of synapses upon thin dendrites of the ganglion cell. Bundles of axons (*ax*) are not immunoreactive. × 600.

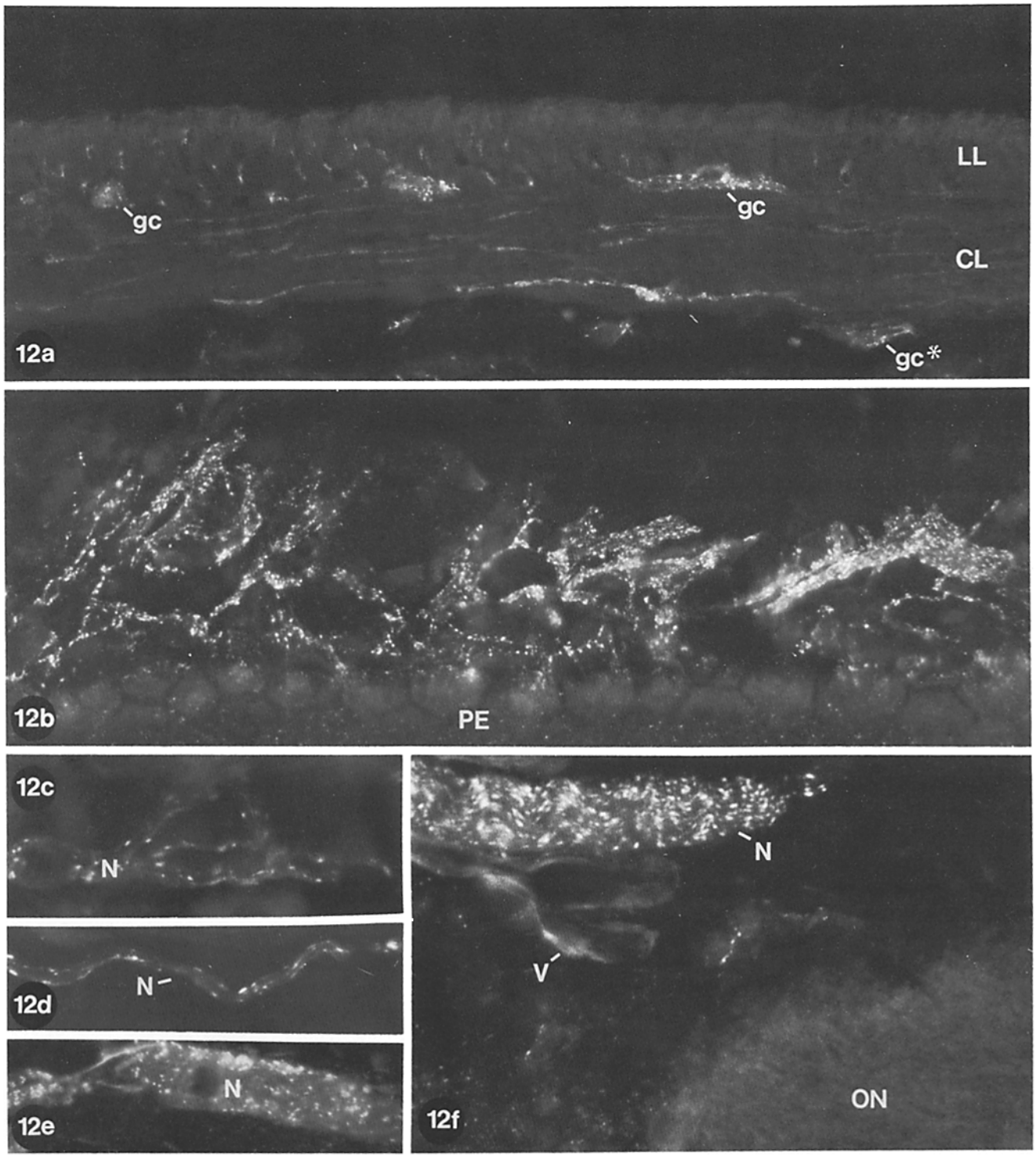

FIGURE 12 Fluorescence micrographs showing distribution of synapsin I immunoreactivity in several types of peripheral nervous tissue of the rat. 10-μm-thick frozen sections. (*a*) Cross section of the small intestine showing the smooth muscle layers (*LL*, longitudinal layer; *CL*, circular layer). Since immunoreactive varicose fibers are oriented parallel to the smooth muscle cells, they are clearly visible as long threads in the circular layer, but appear only as dots in the cross section of the longitudinal layer. Synapses on ganglionic cells of the Auerbach plexus (*gc*) and on the submucosal plexus of Meissner (*gc**) are also visible. (*b*) Immunoreactive varicose fibers around the blood vessels of the choroid of the eye. *PE*, pigmented epithelium cut obliquely. (*c*) Small immunoreactive peripheral nerve in the exocrine pancreas. (*d–f*) Immunoreactive peripheral branches of autonomic nerves in the connective tissue behind the eye. Note: in *c–f*, the immunoreactivity on nerves (*N*) appears as little dots or short rods. In *f*, a weak nonspecific fluorescence (also seen with nonimmune serum) is visible on the optic nerve (*ON*) and on the walls of blood vessels (*v*). *a*, × 210. *b*, × 448. *c*, × 1,168. *d*, × 928. *e*, × 448. *f*, × 448.

ferent depths throughout the section. In contrast, plastic sections, which can accommodate only one layer of synapses, should provide a faithful image of the density of immunoreactive synapses. Due to the limited resolution power of the light microscope and to the nature of the immunostain (nonimmunoreactive synapses are not visible), one cannot establish from our fluorescent images whether synapsin I is or is not present at all synapses of the neuropile in the central nervous system. (An immunocytochemical study at the electron microscopic level to solve this problem is reported in an accompanying paper [10].) However, our images are compatible with the possibility that most or all synapses (with the possible exception of synapses involving very specialized neurons such as photoreceptor cells in the retina) contain synapsin I.

THE IMMUNOHISTOCHEMICAL PROCEDURE USED: Results analogous to those reported in this paper were obtained when frozen and plastic tissue sections, adjacent to those used for synapsin I localization by immunofluorescence, were used to stain synapsin I by an indirect immunoperoxidase procedure (not shown). The only noticeable difference between the two types of immunostain was that regional variations in the intensity of the immunostain appeared to be amplified by the peroxidase procedure (an effect reminiscent of that produced by high-contrast paper in photography). For instance, prominent peroxidase reaction product was visible at the large mossy fiber terminals in sections of the hippocampus under experimental conditions in which the small synapses of the strata oriens and radiatum were still devoid of any reaction product.

Immunostain of frozen sections was the technique of choice when a substantial depth of field was desired (see, for instance Fig. 10 *main field* and *bottom-right inset*). Plastic sections, on the contrary, were used when it was necessary to obtain a high resolution of histological details. In plastic sections, synapsin I remained immunoreactive in spite of the denaturing steps involved in Epon embedding and Epon removal (17, 31, 33). Thus, plastic tissue sections, which have been used in immunocytochemistry primarily to localize secretory proteins (1, 2, 13, 34, 39, 47), seem to be suitable for the study of the localization of cytoplasmic proteins, at least when they are present in cells (or in cell compartments) at high concentrations. The concentration of synapsin I at synapses appears to be very high (18, 24).

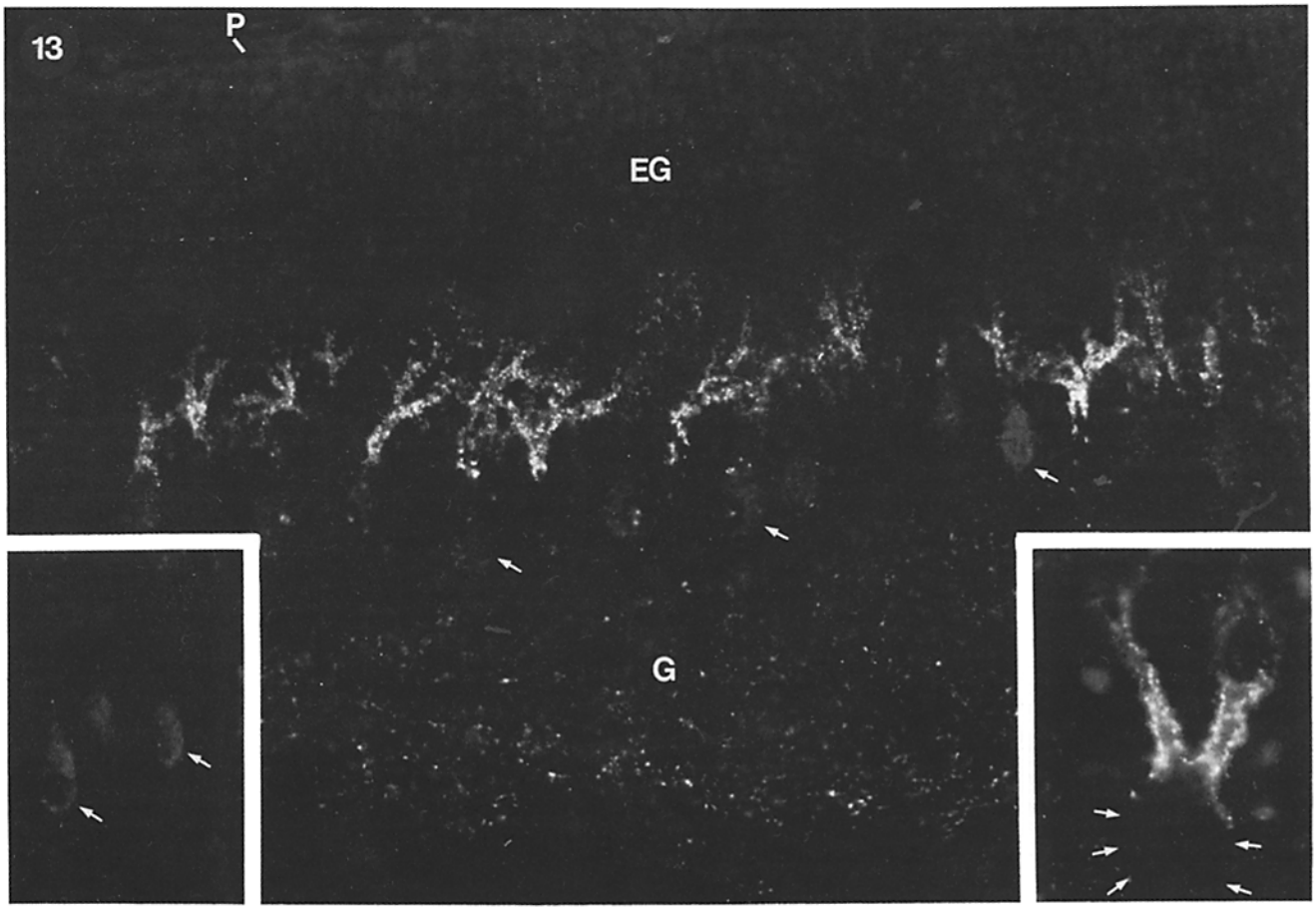

FIGURE 13 Fluorescence micrograph illustrating the distribution of synapsin I immunoreactivity in the developing chick cerebellum. 10-μm-thick frozen sections of chick cerebellum at embryonic day 17. *Main field:* A weak nonspecific staining allows identification of the main features of the cerebellar cortex at this stage of development. *P*, pial surface; *EG*, external granule layer; *G*, granule layer. Immunoreactive dots outline the profiles of primary dendrites of Purkinje cells. Our images correspond very closely to previous descriptions of Purkinje cells at this stage of development in the chick. They have been described as looking "like a bunch of flowers in a Chianti flask" (35). Only sparse dots of immunoreactive material are visible in the granule layer. The *right inset* shows a higher magnification of one Purkinje cell with two primary dendrites. The *left inset* shows a section processed by the same immunostaining procedure used for the main picture but in which rabbit antiserum directed against synapsin I was replaced by preimmune serum. Arrows in the main field and in the two insets point to Purkinje cell perikarya. × 396; *right inset*, × 960; *left inset*, × 396.

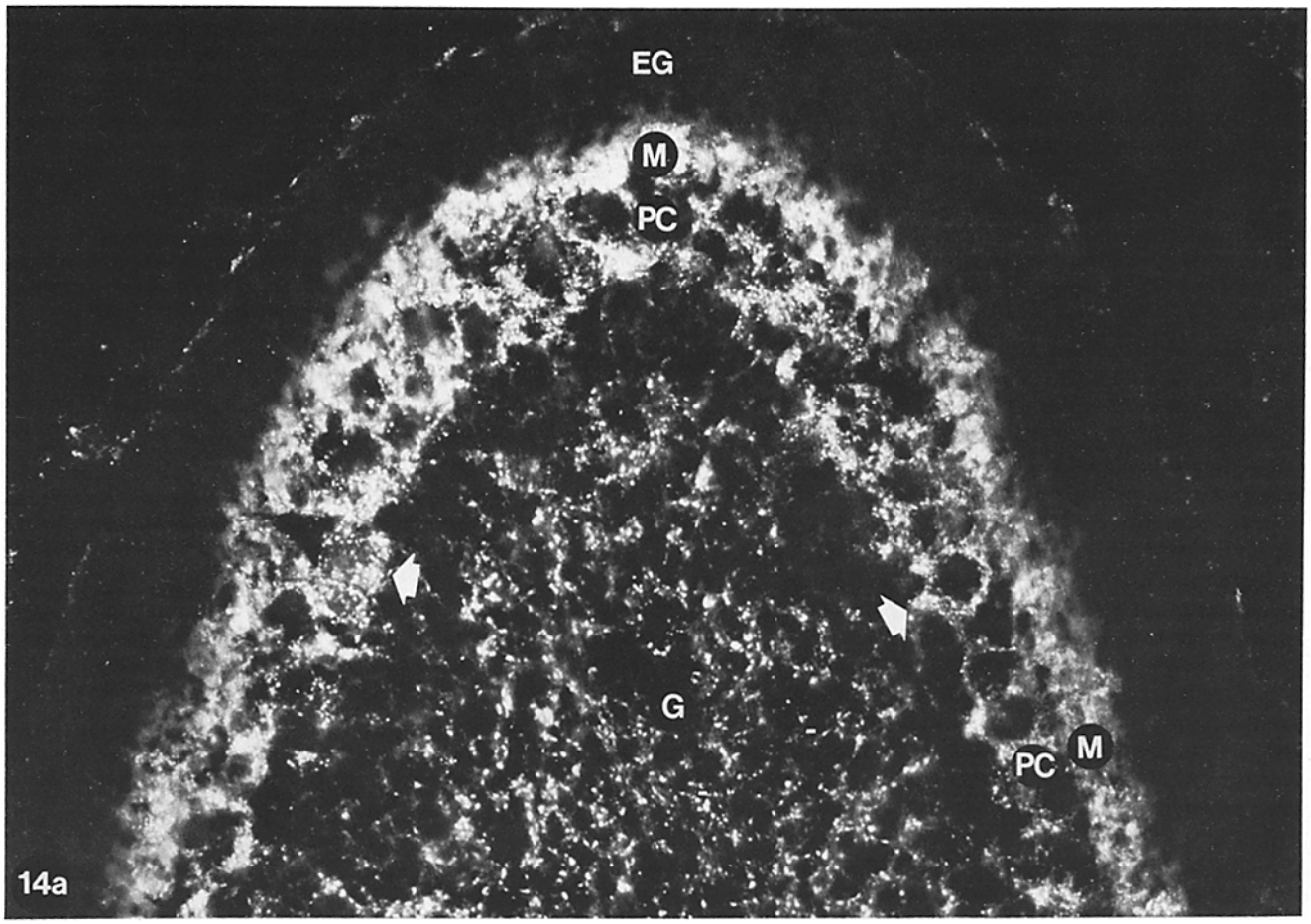

14a

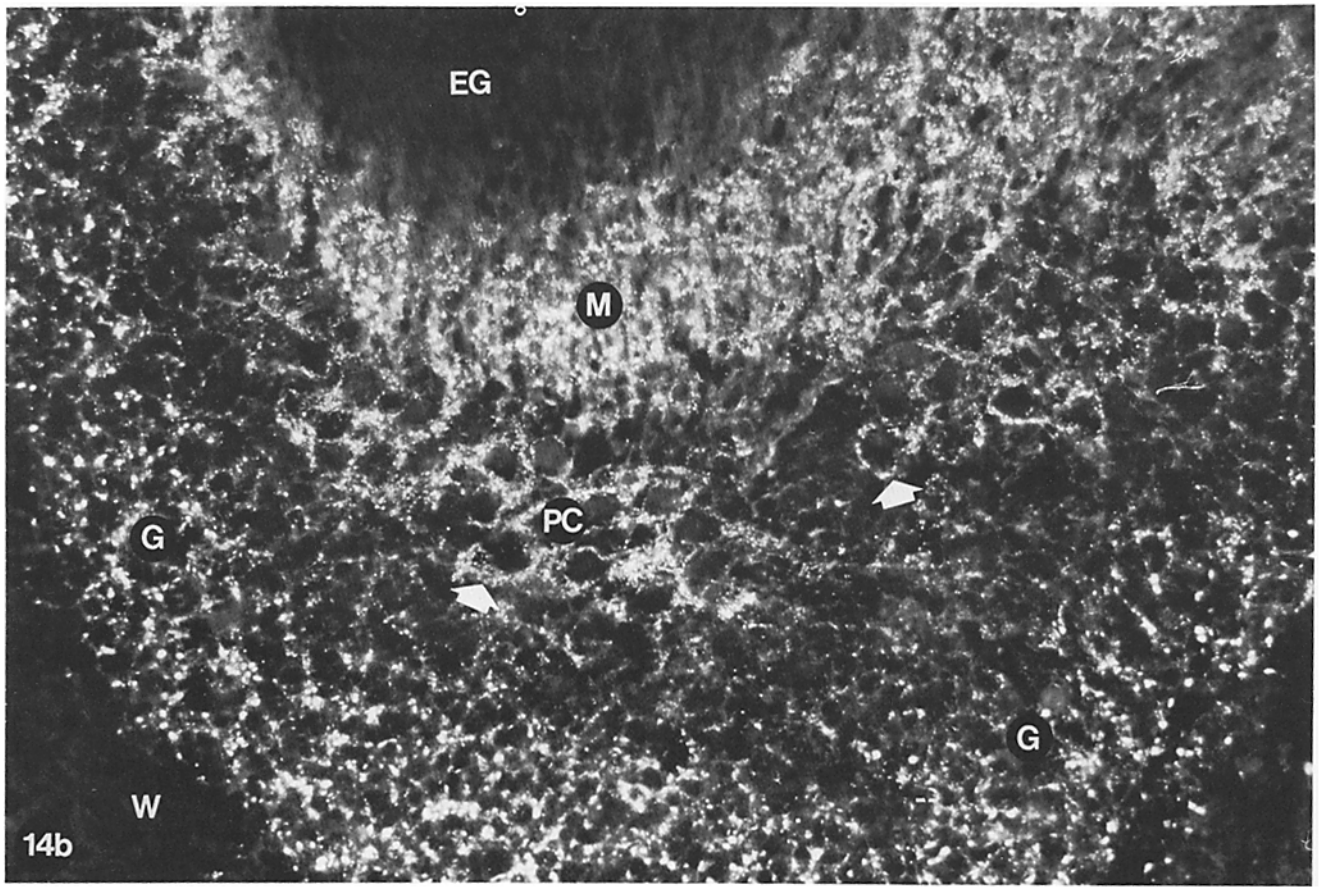

14b

RESULTS AND DISCUSSION

Compartmentalization of Synapsin I in the Nervous System

Immunofluorescent images clearly suggest that synapsin I is concentrated in the synaptic region of nerve cells, but in most cases do not allow identification of the precise localization of synapsin I in the synapse. In all regions of the nervous system examined, however, the fluorescent pattern obtained by anti-synapsin I immunostaining was compatible with a localization of synapsin I in the presynaptic compartment of the synaptic junction, in agreement with results obtained in electron microscopic studies (10). Furthermore, at synapses where the nerve ending is known to be very large, synapsin I immunoreactivity appeared to be concentrated at the portion of the ending abutting the synaptic junction. (See, for instance, the localization of immunoreactivity corresponding to hippocampal mossy fiber terminals in Fig. 7 *a*, and the distribution of synapsin I immunoreactivity in the nerve ending of the motor end plate in the top left inset of Fig. 10.) This compartmentalization of synapsin I in nerve endings is compatible with a specific association of synapsin I with synaptic vesicles, as suggested by parallel electron microscopic and subcellular fractionation studies (10, 24).

In the overwhelming majority of neurons, synapsin I immunoreactivity could not be detected in cell bodies, dendrites, or the preterminal portion of axons. This indicates that, in the large majority of cell bodies and axons, synapsin I does not reach the critical concentration required to allow detection by our conditions of immunostaining. However, synapsin I is undoubtedly present in cell bodies, since the biochemical machinery needed to synthesize cytoplasmic proteins is not present in the nerve endings (41). Similarly, it must be present in the preterminal portion of axons, en route from the cell bodies to the terminals. In fact, experiments involving nerve ligation have demonstrated that, upon local block of axoplasmic transport, synapsin I becomes immunohistochemically detectable (in the form of discrete dots) in the portions of axons close to the ligature (15). The punctate appearance of synapsin I at these regions suggests that, in axons, too, synapsin I is bound to particulate structures. The temporal and topographical patterns of accumulation of synapsin I at sites of nerve ligation correlate with the temporal and topographical accumulation of synaptic vesicle-associated antigens (15). This observation is consistent with the possibility that synapsin I migrates down axons in association with synaptic vesicles. The number of synapsin I molecules on individual vesicles is probably not sufficient to produce a visible signal under our experimental conditions. Interestingly, a distribution of immunoreactivity similar to that observed for synapsin I (staining of synapses but not of axons, cell bodies, or dendrites) was observed for a protein that appears to be an intrinsic membrane protein of the synaptic vesicle (32).

A punctate pattern of synapsin I immunoreactivity can also be observed along the peripheral branches of nonsomatic nerves. Similar images have been observed in these peripheral nerves by staining for neurotransmitters (49). They probably correspond to focal accumulations of synaptic vesicles (49). Thus, in this case, too, the presence of synapsin I seems to correlate with the presence of synaptic vesicles.

General Comments

The images presented in this paper contribute towards an understanding of the function of synapsin I. The demonstration that synapsin I is widely distributed in synapses of the central and peripheral nervous system indicates that synapsin I plays a general role in synaptic function. The appearance of synapsin I in parallel with synaptogenesis (establishment of synaptic contacts among nerve cells [25]) rather than with neurogenesis (generation of nerve cells [25]), during ontogenesis of the nervous system stresses the close link between synapsin I and the physiology of the nerve ending. This link is also indicated by the absence of synapsin I from the cells of the adrenal medulla (11, 15); these cells are related to neurons but are not bona fide neurons since they lack axons and axon terminals.

The function of synapsin I is still unknown. The results of this paper are consistent with the possibility (suggested by the results of the accompanying papers [10, 24]) that synapsin I participates in synaptic vesicle function. Given the very specific restriction of synapsin I to nerve cells, it probably participates in some regulatory process that is not shared by secretory vesicles of nonneuronal cells.

The unique localization of synapsin I indicates that this protein may be extremely useful in morphological as well as biochemical studies as a marker for synapses.

We thank Dr. G. E. Palade for encouragement and discussion throughout the work. We also thank Drs. S. I. Walaas and T. Hokfelt for discussion, F. D. Wilson for help in purifying synapsin I, A. Villa for help in experiments on the neuromuscular junction, P. Ossorio and S. M. Harris for photographic assistance, and A. E. Gwardyak for typing the manuscript.

This work was supported by National Institutes of Health–Institutional Biomedical Research Support grant RR-05358 and by a Muscular Dystrophy grant to P. De Camilli and by U.S. Public Health Service grants MH-17387 and NS-08440 and a grant from the McKnight Foundation to P. Greengard.

FIGURE 14 Fluorescence micrographs illustrating the distribution of synapsin I immunoreactivity in the developing rat cerebellum. 10-μm-thick sagittal frozen sections of cerebellar cortex at postembryonic day 9. (*a*) Apex of a cerebellar cortical fold. Note the four layers recognizable at this stage in the cerebellar cortex (25). *G*, granule cell layer; *PC*, Purkinje cell layer; *M*, molecular layer; *Eg*, external granule layer. Immunoreactive dots present in the granule cell layer appear quite disperse when compared with the large dots visible on the mature glomeruli in the granule cell layer of the adult cerebellum (Fig. 3 *a*). Purkinje cell perikarya are densely covered by synapses. Two thick arrows in the figure point to a tangentially sectioned (*left*) and to a cross-sectioned (*right*) Purkinje cell body, respectively. Immunoreactive synapses (poorly resolved in this picture) are present on the immature dendrites of Purkinje cells in the rudimentary molecular layer. No immunoreactivity is present on the external granule layer, which does not contain synapses. (*b*) Concave portion of a cerebellar cortical fold in a region of the cerebellum posterior to the one shown in *a*. The features of this region are very similar to the features of the region shown in *a*, with the exception that Purkinje cell perikarya are still organized in multiple layers. This corresponds to a slightly earlier stage of development and is in agreement with the known anterior posterior gradient of cerebellar maturation in the rat (29). *W*, region that will correspond to the white matter in the adult cerebellum. Other labeling as in *a*. *a*, × 409. *b*, × 345.

Received for publication 20 August 1982, and in revised form 29 December 1982.

REFERENCES

1. Baskin, D. G., S. L. Erlandsen, and J. A. Parsons. 1979. Influence of hydrogen peroxide or alcoholic sodium hydroxide on the immunocytochemical detection of growth hormone and prolactin after osmium fixation. *J. Histochem. Cytochem.* 27:1290–1292.
2. Bendayan, M., J. Roth, A. Perrelet, and L. Orci. 1980. Quantitative immunocytochemical localization of pancreatic secretory proteins in subcellular compartments of the rat acinar cell. *J. Histochem. Cytochem.* 28:149–160.
3. Bloom, W., and D. W. Fawcett. 1975. A Textbook of Histology, 10th ed. W. B. Saunders Company, Philadelphia.
4. Bloom, F. E., T. Ueda, E. Battenberg, and P. Greengard. 1979. Immunocytochemical localization, in synapses, of protein I, an endogenous substrate for protein kinases in mammalian brain. *Proc. Natl. Acad. Sci. USA* 76:5982–5986.
5. Browning, M. D., C-K. Huang, and P. Greengard. 1982. Biological similarity of two phosphoproteins (proteins IIIa and IIIb) associated with synaptic vesicles in rat brain. *Soc. Neurosci. Abstr.* 8:794.
6. Conradi, S. 1969. Ultrastructure and distribution of neuronal and glial elements on the motor neuron surface in the lumbosacral spinal cord of the adult rat. *Acta Physiol. Scand. Suppl.* 332:5–48.
7. Couteaux, R. 1947. Contribution a l'étude de la synapse myoneurale. *Rev. Can. Biol.* 6:563–711.
8. Daw, N. 1982. Selective staining of photoreceptors. *Trends Neurosci.* 5:33–34.
9. De Camilli, P., R. Cameron, and P. Greengard. 1980. Localization of protein I by immunofluorescence in the adult and developing nervous system. *J. Cell Biol.* 87 (2, Pt. 2): 72 *a* (Abstr.).
10. De Camilli, P., S. M. Harris, W. B. Huttner, and P. Greengard. 1982. Synapsin I (protein I), a nerve terminal-specific phosphoprotein. II. Its specific association with synaptic vesicles demonstrated by immunocytochemistry in agarose-embedded synaptosomes. *J. Cell Biol.* 96:1355–1373.
11. De Camilli, P., T. Ueda, F. E. Bloom, E. Battenberg, and P. Greengard. 1979. Widespread distribution of protein I in the central and peripheral nervous systems. *Proc. Natl. Acad. Sci. USA* 76:5977–5981.
12. Dolphin, A. C., and P. Greengard. 1981. Serotonin stimulates phosphorylation of protein I in the facial motor nucleus of rat brain. *Nature (Lond.).* 289:76–79.
13. Erlandsen, S. L., J. A. Parsons, and C. B. Rodning. 1979. Technical parameters of immunostaining of osmicated tissue in epoxy sections. *J. Histochem. Cytochem.* 27:1286–1289.
14. Forn, J., and P. Greengard. 1978. Depolarizing agents and cyclic nucleotides regulate the phosphorylation of specific neuronal proteins in rat cerebral cortex slices. *Proc. Natl. Acad. Sci. USA* 75:5195–5199.
15. Fried, G., E. J. Nestler, P. De Camilli, L. Stjärne, L. Olson, J. M. Lundberg, T. Hökfelt, C. C. Ouimet, and P. Greengard. 1982. Cellular and subcellular localization of protein I in the peripheral nervous system. *Proc. Natl. Acad. Sci. USA* 79:2717–2721.
16. Gerace, L., A. Blum, and G. Blobel. 1978. Immunocytochemical localization of the major polypeptides of the nuclear pore complex-lamina fraction. I. Interphase and mitotic distribution. *J. Cell Biol.* 79:546–566.
17. Glauert, A. M. 1975. Practical Methods in Electron Microscopy: Fixation, Dehydration and Embedding of Biological Specimens. American Elsevier, New York.
18. Goelz, S. E., E. J. Nestler, B. Chehrazi, and P. Greengard. 1981. Distribution of protein I in mammalian brain as determined by a detergent-based radioimmunoassay. *Proc. Natl. Acad. Sci. USA* 78:2130–2134.
19. Heimer, L., R. D. Switzer, and G. W. Van Hoesen. 1982. Ventral striatum and ventral pallidum. Components of the motor system? *Trends Neurosci.* 5:83–87.
20. Heimer, L., and R. D. Wilson. 1975. The subcortical projections of the allocortex: similarities in the neural associations of the hippocampus, the piriform cortex and the neocortex. *In* Golgi Centennial Symposium. M. Santini, editor. Raven Press, New York. 177–193.
21. Huang, C.-K., M. D. Browning, and P. Greengard. 1982. Purification and characterization of protein IIIb, a mammalian brain phosphoprotein. *J. Biol. Chem.* 257:6524–6528.
22. Huttner, W. B., L. J. DeGennaro, and P. Greengard. 1981. Differential phosphorylation of multiple sites in purified protein I by cyclic AMP-dependent and calcium-dependent protein kinases. *J. Biol. Chem.* 256:1482–1488.
23. Huttner, W. B., and P. Greengard, 1979. Multiple phosphorylation sites in protein I and their differential regulation by cyclic AMP and calcium. *Proc. Natl. Acad. Sci. USA* 76:5402–5406.
24. Huttner, W. B., W. Schiebler, P. Greengard, and P. De Camilli. 1982. Synapsin I (protein I), a nerve terminal-specific phosphoprotein. III. Its association with synaptic vesicles studied in a highly purified synaptic vesicle preparation. *J. Cell Biol.* 96:1374–1388.
25. Jacobson, M. 1978. Developmental Neurobiology. 2nd ed., Plenum Press, New York.
26. Johnson, E. M., T. Ueda, H. Maeno, and P. Greengard. 1972. Adenosine 3',5'-monophosphate-dependent phosphorylation of a specific protein in synaptic membrane fractions from rat cerebrum. *J. Biol. Chem.* 247:5650–5652.
27. Kennedy, M. B., and P. Greengard. 1981. Two calcium/calmodulin-dependent protein kinases, which are highly concentrated in brain, phosphorylate protein I at distinct sites. *Proc. Natl. Acad. Sci. USA* 78:1293–1297.
28. Krueger, B. K., J. Forn, and P. Greengard. 1977. Depolarization-induced phosphorylation of specific proteins, mediated by calcium ion influx, in rat brain synaptosomes. *J. Biol. Chem.* 252:2764–2773.
29. Llinas, R., editor. 1969. Proceedings of the First International Symposium of the Institute for Biomedical Research: Neurobiology of Cerebellar Evolution and Development. Institute for Biomedical Research, Chicago.
30. Lowry, O. H., N. J. Rosebrough, A. L. Farr, and R. J. Randall. 1951. Protein measurement with the Folin phenol reagent. *J. Biol. Chem.* 193:265–275.
31. Luft, J. H. 1961. Improvements in epoxy resin embedding methods. *J. Biophys. Biochem. Cytol.* 9:409–414.
32. Matthew, W. D., L. Tsavaler, and L. F. Reichardt. 1981. Identification of a synaptic vesicle-specific membrane protein with a wide distribution in neuronal and neurosecretory tissue. *J. Cell Biol.* 91:257–269.
33. Maxwell, M. H. 1978. Two rapid and simple methods used for the removal of resins from 1.0 μm thick epoxy sections. *J. Microsc. (Lond.).* 112:253–255.
34. Moriarty, G. C. 1973. Adenohypophysis: ultrastructural cytochemistry. A review. *J. Histochem. Cytochem.* 21:855–894.
35. Mugnaini, E. 1969. Ultrastructural studies on the cerebellar histogenesis. II. Maturation of nerve cell populations and establishment of synaptic connections in the cerebellar cortex of the chick. *In* Proceedings of the First International Symposium of the Institute for Biomedical Research: Neurobiology of Cerebellar Evolution and Development. R. Llinas, editor. Institute for Biomedical Research, Chicago. 749–782.
36. Nestler, E. J., and P. Geengard. 1980. Dopamine and depolarizing agents regulate the state of phosphorylation of protein I in the mammalian superior cervical sympathetic ganglion. *Proc. Natl. Acad. Sci. USA* 77:7479–7483.
37. O'Farrell, P. Z., H. W. Goodman, and P. H. O'Farrell. 1977. High resolution two-dimensional electrophoresis of basic as well as acidic proteins. *Cell.* 12:1133–1142.
38. Palay, S. L., and V. Chan-Palay. 1974. Cerebellar Cortex: Cytology and Organization. Springer-Verlag, New York.
39. Pelletier, G., R. Puviani, O. Bosler, and L. Descarries. 1981. Immunocytochemical detection of peptides in osmicated and plastic-embedded tissue. *J. Histochem. Cytochem.* 29:759–764.
40. Perez de la Mora, M., L. D. Possani, R. Tapia, L. Teran, R. Palacios, K. Fuxe, T. Hökfelt, and Å. Ljungdahl. 1981. Demonstration of central γ-aminobutyrate-containing nerve terminals by means of antibodies against glutamate decarboxylase. *Neuroscience.* 6:875–895.
41. Peters, A., S. L. Palay, and H. deF. Webster. 1976. The Fine Structure of the Nervous System: The Neurons and Supporting Cells. W. B. Saunders Company, Philadelphia.
42. Ramon Y Cayal, S. 1911. Histologie du système nerveux de l'homme et des vertebres. Maloine, Paris.
43. Rinvik, E., and I. Grofova. 1970. Observations on the fine structure of the substantia nigra in the cat. *Exp. Brain Res.* 11:229–248.
44. Schaeffer, S. F., and E. Raviola. 1978. Membrane recycling in the cone cell endings of the turtle retina. *J. Cell Biol.* 79:802–825.
45. Shepherd, G. M. 1979. The Synaptic Organization of the Brain. Oxford University Press, New York.
46. Sieghart, W., J. Forn, and P. Greengard. 1976. Ca^{2+} and cyclic AMP regulate phosphorylation of same two membrane-associated proteins specific to nerve tissue. *Proc. Natl. Acad. Sci. USA* 76:2475–2479.
47. Sternberger, L. A. 1979. *Immunocytochemistry.* 2nd ed. J. Wiley & Sons, New York.
48. Swanson, L. W., J. M. Wyss, and W. M. Cowan. 1978. An autoradiographic study of the organization of intrahippocampal association pathway in the rat. *J. Comp. Neurol.* 181:681–716.
49. Thureson-Klein, Å, R. L. Klein, and O. Johansson. 1979. Catecholamine-rich cells and varicosities in bovine splenic nerve, vesicle contents and evidence for exocytosis. *J. Neurobiol.* 10:309–324.
50. Ueda, T., and P. Greengard. 1977. Adenosine 3':5'-monophosphate-regulated phosphoprotein system of neuronal membranes. I. Solubilization, purification, and some properties of an endogenous phosphoprotein. *J. Biol. Chem.* 252:5155–5163.
51. Ueda, T., P. Greengard, K. Berzins, R. S. Cohen, F. Blomberg, D. J. Grab, and P. Siekevitz. 1979. Subcellular distribution in cerebral cortex of two proteins phosphorylated by a cAMP-dependent protein kinase. *J. Cell Biol.* 83:308–319.
52. Walaas, I., and F. Fonnum. 1979. The distribution and origin of glutamate decarboxylase and choline acetyltransferase in ventral pallidum and other basal forebrain regions. *Brain Res.* 177:325–336.
53. Weeke, B. 1973. General remarks on principles, equipment, reagents and procedures. *Scand. J. Immunol.* 2(Suppl. 1):15–35.